

Mathematical analysis of a model for zoonotic visceral leishmaniasis



Nafiu Hussaini^a, Kamaldeen Okuneye^b, Abba B. Gumel^{b,*}

^a Department of Mathematical Sciences, Bayero University Kano, P.M.B. 3011, Kano, Nigeria

^b School of Mathematical and Statistical Sciences, Arizona State University, Tempe, AZ 85287, USA

ARTICLE INFO

Article history:

Received 12 November 2017

Accepted 6 December 2017

Available online 13 December 2017

Keywords:

Leishmania infantum

Zoonotic visceral leishmaniasis (ZVL)

Reproduction number

Stability

Backward bifurcation

ABSTRACT

Zoonotic visceral leishmaniasis (ZVL), caused by the protozoan parasite *Leishmania infantum* and transmitted to humans and reservoir hosts by female sandflies, is endemic in many parts of the world (notably in Africa, Asia and the Mediterranean). This study presents a new mathematical model for assessing the transmission dynamics of ZVL in human and non-human animal reservoir populations. The model undergoes the usual phenomenon of backward bifurcation exhibited by similar vector-borne disease transmission models. In the absence of such phenomenon (which is shown to arise due to the disease-induced mortality in the host populations), the nontrivial disease-free equilibrium of the model is shown to be globally-asymptotically stable when the associated reproduction number of the model is less than unity. Using case and demographic data relevant to ZVL dynamics in Aracatuba municipality of Brazil, it is shown, for the default case when systemic insecticide-based drugs are not used to treat infected reservoir hosts, that the associated reproduction number of the model (\mathcal{R}_0) ranges from 0.3 to 1.4, with a mean of $\mathcal{R}_0 = 0.85$. Furthermore, when the effect of such drug treatment is explicitly incorporated in the model (i.e., accounting for the additional larval and sandfly mortality, following feeding on the treated reservoirs), the range of \mathcal{R}_0 decreases to $\mathcal{R}_0 \in [0.1, 0.6]$, with a mean of $\mathcal{R}_0 = 0.35$ (this significantly increases the prospect of the effective control or elimination of the disease). Thus, ZVL transmission models (in communities where such treatment strategy is implemented) that do not explicitly incorporate the effect of such treatment may be over-estimating the disease burden (as measured in terms of \mathcal{R}_0) in the community. It is shown that \mathcal{R}_0 is more sensitive to increases in sandfly lifespan than that of the animal reservoir (so, a strategy that focuses on reducing sandflies, rather than the animal reservoir (e.g., via culling), may be more effective in reducing ZVL burden in the community). Further sensitivity analysis of the model ranks the sandfly removal rate (by natural death or by feeding from insecticide-treated reservoir hosts), the biting rate of sandflies on the reservoir hosts and the progression rate of exposed reservoirs to active ZVL as the three parameters with the most effect on the disease dynamics or burden (as measured in terms of the reproduction number \mathcal{R}_0). Hence, this study identifies the key parameters that play a key role on the disease dynamics, and thereby contributing in the design of effective control strategies (that target the identified parameters).

© 2017 The Authors. Production and hosting by Elsevier B.V. on behalf of KeAi Communications Co., Ltd. This is an open access article under the CC BY-NC-ND license (<http://creativecommons.org/licenses/by-nc-nd/4.0/>).

* Corresponding author.

E-mail address: agumel@asu.edu (A.B. Gumel).

Peer review under responsibility of KeAi Communications Co., Ltd.

1. Introduction

The protozoan *Leishmania infantum* (syn., *L. chagasi*) is the causative agent of zoonotic visceral leishmaniasis (ZVL) in humans and canine leishmaniasis (CanL) in dogs (Hartemink et al., 2011; Podaliri Vulpiani, Iannetti, Paganico, Iannino, & Ferri, 2011; Ribas, Zaher, Shimozako, & Massad, 2013). The protozoan parasite is transmitted from infected animal hosts (domestic dogs serve as principal reservoirs) to susceptible female sandflies (*Diptera: Phlebotomine*) and then to susceptible humans (who are regarded as dead-end hosts of the disease) (Elnaïem et al., 2001; Hoogstraal & Heyneman, 1969; Hussaini, Lubuma, Barley, & Gumel, 2016; Kirk, 1939; Podaliri Vulpiani et al., 2011; Ribas et al., 2013). ZVL, which is endemic in Africa, Europe (particularly the Mediterranean region) and Asia (particularly the Indian subcontinent) (European Centre for Disease Prevention and Control, ; Podaliri Vulpiani et al., 2011), is an acute and life-threatening emerging disease with estimated yearly incidence in the range 200 000 to 400 000 (Leta, Dao, Mesele, & Alemayehu, 2014; World Health Organization). Furthermore, increase in risk factors associated with climate change and other environmental challenges makes ZVL to be a growing major public health concern (Hartemink et al., 2011).

An adult female sandfly lays about 40 – 70 eggs during a single gonotrophic cycle (these eggs are typically laid in damp dark places in the cattle sheds, animal burrows, tree roots and in soil rich in organic matter) (European Centre for Disease Prevention and Control, ; Sand fly life cycle,). The eggs laid in these micro-habitats hatch into larvae in 4 – 20 days (European Centre for Disease Prevention and Control,). Larvae develop into four instar stages (each one larger than the one before; the newly hatched first instar larvae have two rear bristles, while all later larval developments have four rear bristles) (European Centre for Disease Prevention and Control,). Larvae are mainly scavengers found in moist areas, such as animal burrows, feeding on organic matter (e.g., fungi, decaying leaves and animal faeces) (European Centre for Disease Prevention and Control, ; Sand fly life cycle,). During the fourth molt, the larva matures into a pupa (the whole process of maturation from larvae to pupae takes about 20 – 30 days depending on species, temperature and nutrient availability) (European Centre for Disease Prevention and Control,). Pupae then develop into adult sandflies in about 6 – 13 days (European Centre for Disease Prevention and Control, ; Sand fly life cycle,). Thus, the duration of the whole cycle, from egg laying to an adult sandfly, varies between 30 and 63 days depending on species, temperature and nutrient availability (European Centre for Disease Prevention and Control,). Adult sandflies usually mate within a few days after emerging from the pupal stage, after which the female sandfly moves to quest for blood meal required to produce eggs (European Centre for Disease Prevention and Control,). The feeding activity of the female adult sandfly is influenced by temperature, humidity and air movement (European Centre for Disease Prevention and Control, ; Sand fly life cycle,). Sandflies, which are active and feed during the early morning and evening hours when temperature falls and humidity rises, have an average lifespan of about 14 days (European Centre for Disease Prevention and Control, ; Sand fly life cycle,). A schematic description of the life-cycle of the sandfly is depicted in Fig. 1. Although there is a vaccine against ZVL in animal populations (Canileish) (Canileish, 2017; Vetlife), no such vaccine currently exists for use in humans (although a number of candidate vaccines are at various stages of development and clinical trials) (Gillespie et al., 2016; Kumar & Engwerda, 2014; Mcallister, 2014) (it is however, known that an effective vaccine against leishmaniasis will prompt long-lasting immunity in humans (Bertholet et al., 2009; Gillespie et al., 2016; Mcallister, 2014; Nagill & Kaur, 2011)). Furthermore, although ZVL is curable using drugs such as *miltefosine*, *paromomycin* and *liposomal amphotericin B* (Chappuis et al., 2007), basic anti-ZVL preventive measures (such as personal protection against sandfly bites and sandfly-reduction strategies focused on spraying anti-sandfly insecticides in human and animal reservoir habitats) remain perhaps the most effective method for combating ZVL spread in humans (World Health Organization). Treatment of animal reservoir (with systemic insecticide-based drugs, such as *fipronil*) are implemented in places like Bihar, India (Poché, Grant, & Wang, 2016). An additional benefit of the treatment strategy is that it reduces the

Life cycle of sandfly

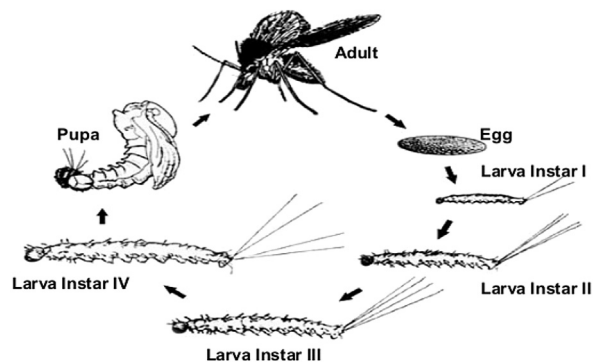


Fig. 1. Schematic diagram of the life-cycle of the sandfly (Sharma,).

number of larvae and adult sandflies who feed on the faeces of (insecticide-based) treated infected reservoirs (Poché et al., 2016).

A number of modeling studies have been carried out to gain insight into ZVL transmission dynamics in human and/or reservoir populations (see, for instance (Burattini, Coutinho, Lopez, & Massad, 1998; Carvalho et al., Hartemink et al., 2011; Hussaini et al., 2016; Ribas et al., 2013; Shimozako, Wu, & Massad, 2017; Zhao et al., 2016), and some of the references therein). Burattini et al. (Burattini et al., 1998). proposed mechanistic model for ZVL transmission within the human and animal reservoir populations, and used the model to evaluate control strategies. Ribas et al. (Ribas et al., 2013). added control terms to the model in (Burattini et al., 1998) to estimate the optimal control strategies for ZVL. Zhao et al. (Zhao et al., 2016). developed a model to describe the ZVL transmission dynamic using a modified SEIR model and the model exhibited backward bifurcation phenomenon. Shimozako et al (Shimozako et al., 2017). updated most of parameters in (Burattini et al., 1998; Ribas et al., 2013) and calculated new value of \mathcal{R}_0 . The current study focuses on the design and analysis of a novel model, which extends some of the aforementioned modeling studies, for assessing the transmission dynamics of ZVL in human and non-human animal reservoir populations. The paper is organized as follows. The model is formulated in Section 2 and rigorously analyzed in Section 3. Sensitivity uncertainty analysis and numerical simulations are reported in Section 4.

2. Model formulation

The model to be developed monitors the transmission dynamics of zoonotic visceral leishmaniasis (ZVL) within the human and animal (reservoir) host populations. Unlike anthroponotic visceral leishmaniasis (which is transmitted from human to vector to human), ZVL is transmitted from infected animals (reservoir) to susceptible vectors (sandflies) and then back to humans. The total human population at time t , denoted by $N_H(t)$, is sub-divided into four compartments of susceptible ($S_H(t)$), infected but not infectious (i.e., asymptotically-infected humans) ($E_H(t)$), symptomatically-infected ($I_H(t)$) and recovered ($R_H(t)$) humans, so that:

$$N_H(t) = S_H(t) + E_H(t) + I_H(t) + R_H(t).$$

Furthermore, the total sandfly population at time t , denoted by $N_V(t)$, is split into two main classes of immature and mature adult female *phlebotomine* sandfly classes. The total immature sandfly population at time t , denoted by $N_{VI}(t)$, consists of the first three stages of sandfly life-cycle (i.e., eggs ($E_V(t)$), larvae ($L_V(t)$) and pupae ($P_V(t)$)). Further, the total mature female sandfly population at time t , denoted by $N_{VM}(t)$, is split into compartments for susceptible female sandflies ($S_V(t)$) and infected female sandflies ($I_V(t)$), so that

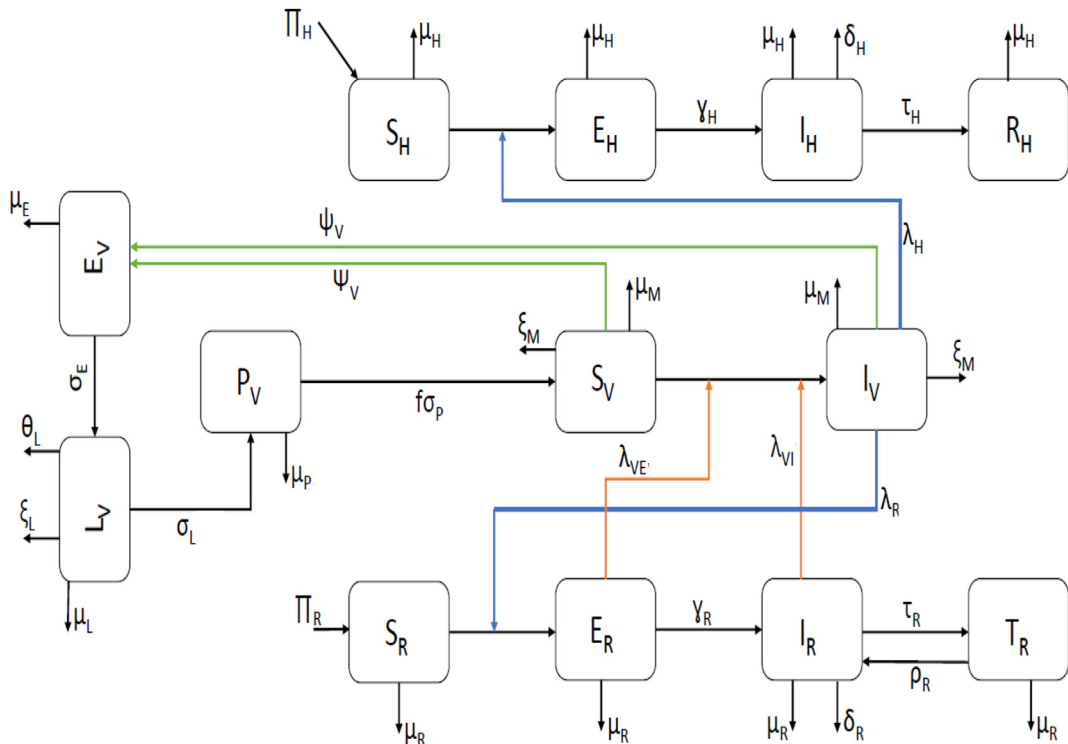


Fig. 2. Flow chart of model (2.1), where $\lambda_H = \frac{\beta_H b_H \mu_V}{N_H + N_R}$, $\lambda_R = \frac{\beta_V b_R \mu_V}{N_H + N_R}$, $\lambda_{VI} = \frac{\beta_V b_R \mu_V}{N_H + N_R}$, $\lambda_{VE} = \frac{\beta_V b_H \mu_V}{N_H + N_R}$.

$$N_V(t) = N_{VI}(t) + N_{VM}(t) = E_V(t) + L_V(t) + P_V(t) + S_V(t) + I_V(t).$$

Finally, the total animal reservoir population at time t , denoted by $N_R(t)$, is sub-divided into compartments for susceptible ($S_R(t)$) exposed ($E_R(t)$), infected ($I_R(t)$) and treated ($T_R(t)$) reservoirs, so that

$$N_R(t) = S_R(t) + E_R(t) + I_R(t) + T_R(t).$$

The model for ZVL transmission in human and reservoir animal populations is given by the following deterministic system of non-linear differential equations (a flow diagram of the model is depicted in Fig. 2; the state variables and parameters of the model are described in Tables 1 and 2, respectively):

$$\begin{aligned} \frac{dS_H}{dt} &= \Pi_H - \frac{\beta_H b_H I_V}{N_H + N_R} S_H - \mu_H S_H, \\ \frac{dE_H}{dt} &= \frac{\beta_H b_H I_V}{N_H + N_R} S_H - (\gamma_H + \mu_H) E_H, \\ \frac{dI_H}{dt} &= \gamma_H E_H - (\tau_H + \mu_H + \delta_H) I_H, \\ \frac{dR_H}{dt} &= \tau_H I_H - \mu_H R_H, \\ \frac{dE_V}{dt} &= \psi_V \left(1 - \frac{N_{VM}}{K_M} \right) (S_V + I_V) - (\sigma_E + \mu_E) E_V, \\ \frac{dL_V}{dt} &= \sigma_E E_V - (\sigma_L + \mu_L + \xi_L + r_L L_V) L_V, \\ \frac{dP_V}{dt} &= \sigma_L L_V - (\sigma_P + \mu_P) P_V, \\ \frac{dS_V}{dt} &= \sigma_P f P_V - \frac{\beta_V b_R (\eta_R E_R + I_R)}{N_H + N_R} S_V - (\mu_M + \xi_M) S_V, \\ \frac{dI_V}{dt} &= \frac{\beta_V b_R (\eta_R E_R + I_R)}{N_H + N_R} S_V - (\mu_M + \xi_M) I_V, \\ \frac{dS_R}{dt} &= \Pi_R - \frac{\beta_R b_R I_V}{N_H + N_R} S_R - \mu_R S_R, \\ \frac{dE_R}{dt} &= \frac{\beta_R b_R I_V}{N_H + N_R} S_R - (\gamma_R + \mu_R) E_R, \\ \frac{dI_R}{dt} &= \gamma_R E_R + \rho_R T_R - (\tau_R + \mu_R + \delta_R) I_R, \\ \frac{dT_R}{dt} &= \tau_R I_R - (\rho_R + \mu_R) T_R. \end{aligned} \tag{2.1}$$

In the model (2.1), Π_H (Π_R) is the recruitment rate for human (reservoir), b_H (b_R) is the biting rate of adult female sandflies on the human (reservoir) host, β_H (β_R) is the probability of infection *per* bite from an infected adult female sandfly (human) to

Table 1
Description of the variables of the model (2.1).

Variable	Interpretation
$S_H(t)$	Population of susceptible humans
$E_H(t)$	Population of humans exposed to ZVL
$I_H(t)$	Population of humans with clinical symptoms of ZVL
$R_H(t)$	Population of humans who recovered from ZVL
$E_V(t)$	Population of sandfly eggs
$L_V(t)$	Population of sandfly larvae
$P_V(t)$	Population of sandfly pupae
$S_V(t)$	Population of susceptible adult female sandflies
$I_V(t)$	Population of ZVL-infected adult female sandflies
$S_R(t)$	Population of susceptible ZVL reservoirs
$E_R(t)$	Population of reservoirs exposed to ZVL
$I_R(t)$	Population of infected reservoirs with clinical symptoms of ZVL
$T_R(t)$	Population of ZVL-treated reservoirs

Table 2
Description of parameters of the model (2.1).

Parameter	Interpretation
$\Pi_H(\Pi_R)$	Recruitment rate of humans (reservoirs)
$\mu_H(\mu_R)$	Natural death rate of humans (reservoirs)
ψ_V	Oviposition rate
$\mu_E, \mu_L, \mu_P, \mu_M$	Natural death rate of eggs, larvae, pupae and adult sandflies, respectively
$\beta_H(\beta_R)$	Transmission probability from infected sandflies to susceptible human (reservoir) hosts
β_V	Transmission probability from infected reservoirs to susceptible sandflies
$b_H(b_R)$	Per capita biting rate of sandflies on the human (reservoir) hosts
$\gamma_H(\gamma_R)$	Progression rate of exposed human (reservoir) hosts to active ZVL class
$\tau_H(\tau_R)$	Treatment rates of human (reservoir) hosts
σ_E	Average maturation rate from eggs to larvae
σ_L	Average maturation rate from larvae to pupae
σ_P	Average maturation rate from pupae to adult sandflies
ρ_R	Rate of relapse of treated reservoirs
K_M	Carrying capacity of adult sandflies
η_R	Modification parameter for relative of infectiousness of reservoirs
f	Fraction of newly-emerged sandflies that are females
$\delta_H(\delta_R)$	Disease-induced death rates of human (reservoir) hosts
$\xi_L(\xi_M)$	Additional death rate of larvae (adult sandflies) due to feeding on faeces of treated reservoir

a susceptible human (sandfly), β_V is the probability of infection *per* bite from an infected reservoir to a susceptible adult female sandfly, $\mu_H(\mu_R)$ is the natural death rate in humans (reservoir hosts) and η_R accounts for the reduction of infectiousness of exposed reservoirs. Laboratory experiments by Laurenti et al. (Laurenti et al., 2013), show that asymptomatic reservoir transmits ZVL to susceptible sandflies at a rate greater than that of symptomatic reservoir hosts (i.e., $\eta_R > 1$). The parameter $\gamma_H(\gamma_R)$ measures the rate at which humans (reservoir hosts) in the $E_H(E_R)$ class develop clinical symptoms of ZVL, while the parameter $\tau_H(\tau_R)$ measures the treatment rate of symptomatic humans (reservoir hosts). The parameters δ_R and ρ_R account, respectively, for the disease-induced death rate and failure rate of treatment received by infected reservoir hosts. It is assumed that recovery confers permanent immunity against ZVL re-infection in humans (Roberts, 2005).

Eggs are laid by adult female sandflies (usually on the surface an organic matter), assumed to be at a logistic rate $\psi_V \left[1 - \frac{N_{VM}(t)}{K_M} \right]$ (where $K_M > N_{VM}(t)$ for all t is the carrying capacity of female adult sandflies and ψ_V is the egg deposition rate). Eggs hatch into the larvae (at a rate σ_E) which, in turn, mature into pupae (at a rate σ_L) and, finally, pupae mature into adult female sandflies (at a rate σ_P). Susceptible adult female sandflies acquire ZVL infection (at the rate $\lambda_{VE} + \lambda_{VI}$, as defined in the caption of Fig. 2) and suffer natural death (at a rate μ_M). Furthermore, adult female sandflies die due to feeding on infected reservoir hosts that have been treated with systemic insecticide-based drugs (Poché et al., 2016) (at a rate ξ_M).

The parameters μ_E, μ_L and μ_P represent, respectively, the natural death rate for eggs, larvae and pupae, while r_{LV} is the density-dependent mortality rate for larvae (accounting for the cannibalism that occurs during larval competition for resources (nutrients) and space) (Poché et al., 2016; Srinivasan & Panicker, 1992). Finally, as in the case of adult sandflies, larvae also suffer additional mortality by feeding on organic material from (insecticide-based) treated infected reservoir hosts, at a rate ξ_L (Poché et al., 2016). Following (Poché et al., 2016), the parameters ξ_L and ξ_M are defined, respectively, as:

$$\xi_L = 0.567e^{-0.073(D_{PT}-1)-0.00545D_{PD}} \quad \text{and} \quad \xi_M = 0.515e^{-0.094D_{PT}},$$

where, D_{PT} is the number of days of post-treatment of infected reservoir and D_{PD} is the number of post-defecation days of reservoir. The model (2.1) accounts for the conservation law of sandfly bites on human and reservoir hosts (the consequence of which is that the human (and reservoir) hosts are always sufficient in abundance and the total number of bites made by sandflies balances the total number of bites received by the human (and reservoir) hosts; see also (Bergsman, Hyman, & Manore, 2016; Bowman, Gumel, van den Driessche, Wu, & Zhu, 2005; Cruz-Pacheco, Esteva, & Vargas, 2012; Marini, Rosá, Pugliese, & Heesterbeek, 2017; Subramanian, Singh, & Sarkar, 2015) for models of similar diseases with one vector and multiple hosts).

Some of the main assumptions made in the formulation of the model (2.1) are:

- (i) Humans are dead-end hosts (i.e., they acquire, but do not transmit, ZVL infection) (Hartemink et al., 2011).
- (i) Humans who recovered from ZVL infection acquire permanent immunity against re-infection (i.e., $\tau_H \neq 0$) (Roberts, 2005).
- (ii) Treated infected reservoir hosts do not usually get cured but develop an immune response that prevents them from becoming infectious (Baneth & Shaw, 2002; Espejo, Costard, & Zagnutt, 2015).
- (iii) Treated reservoir hosts can relapse to active ZVL class due to treatment failure (i.e., $\rho_R \neq 0$) (Petersen & Barr, 2009; Quinnell & Courtenay, 2009).
- (iv) Recovery confers permanent immunity against ZVL re-infection in humans (Hussaini et al., 2016).

Table 3
Human reported ZVL cases in Aracatuba municipality, Brazil (Shimozako et al., 2017).

year	Number of cases	Cumulative cases
1999	15	15
2000	12	27
2001	29	58
2002	52	110
2003	40	150
2004	41	191
2005	16	207
2006	20	227
2007	42	269
2008	27	296
2009	15	311
2010	4	315
2011	5	321
2012	6	327
2013	3	330
2014	12	342
2015	4	346

(v) No direct transmission between reservoirs or between sandflies is assumed (Hartemink et al., 2011).

The model (2.1) extends the deterministic models for ZVL transmission developed in (Burattini et al., 1998; Ribas et al., 2013; Shimozako et al., 2017; Zhao et al., 2016) by, *inter alia*,

- (a) adding the compartments of immature sandflies (i.e., the compartments E_V , L_V and P_V).
- (b) allowing for the relapse of treated reservoir hosts to active ZVL class due to treatment failure (i.e., $\rho_R \neq 0$).
- (c) adding density-dependent larval mortality (i.e., $r_L \neq 0$).
- (d) allowing for additional mortality of sandfly larvae (i.e., $\xi_L \neq 0$) and adult female sandfly ($\xi_M \neq 0$) due to feeding on the faeces of treated infected reservoir hosts.
- (e) using varying total populations of the human and reservoir hosts (constant population was used in (Burattini et al., 1998; Ribas et al., 2013; Shimozako et al., 2017)).

The model (2.1) is, first of all, fitted using the ZVL case and demographic data from Aracatuba municipality, Brazil for the period 1999 – 2015 (tabulated in Table 3) (Centre of Epidemiological Surveillance of Sao Paulo State (CES-SP) and Brazil, 2016; Shimozako et al., 2017). The results obtained, depicted in Fig. 3, show a reasonably good fit to the data (expressed in terms of cumulative number of yearly cases). It is worth mentioning that, for the model fitting, the human demographic parameters (Π_H and μ_H) are parameterize as follows. Since the average total population of Aracatuba municipality is 180,000 (see Table 3), and the average lifespan in Brazil is 75 years (World Bank et al., 2015) (i.e., $1/\mu_H = 75$ years, so that $\mu_H = 3.65 \times 10^{-5}$ per day), it follows from the relation $\Pi_H/\mu_H = 180,000$ that $\Pi_H = 6.575$ per day. Furthermore, since systemic insecticide-based drugs were not used to treat infected reservoir hosts in Aracatuba municipality, Brazil during the period 1999 to 2015, the

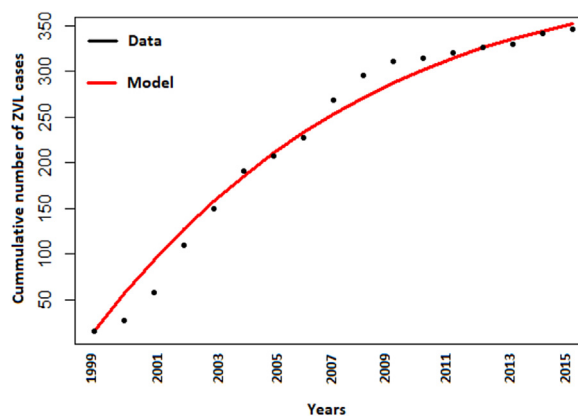


Fig. 3. Comparison of observed ZVL cumulative data from Aracatuba municipality, Brazil (dotted lines) and model prediction (solid curve). Parameter values used are as given in Table 4, with $\xi_L = \xi_M = 0$ and the following initial conditions: $S_H(0) = 176000$; $E_H(0) = 4000$; $I_H(0) = 15$; $R_H(0) = 9$; $E_V(0) = 1000$; $L_V(0) = 100$; $P_V(0) = 50$; $S_V(0) = 10$; $I_V(0) = 1000$; $S_R(0) = 2000$; $E_R(0) = 300$; $I_R(0) = 100$; $T_R(0) = 10$.

Table 4
Values and ranges of the parameters of the model (2.1).

Parameter	Range	Baseline	Reference
Π_H	4 – 7 day ⁻¹	6 day ⁻¹	(World Bank ata, 2015)
μ_H	$3.67 \times 10^{-5} - 5.07 \times 10^{-5}$ day ⁻¹	3.67×10^{-5} day ⁻¹	(World Bank ata, 2015)
b_R	0.03 – 0.2	0.16	(Hartemink et al., 2011; Shimozako et al., 2017)
β_H	0.2 – 0.8	0.56	(Hartemink et al., 2011; Zhao et al., 2016)
δ_H	$2.37 \times 10^{-4} - 5.03 \times 10^{-4}$ day ⁻¹	0.0003 day ⁻¹	(Stauch et al., 2011; Zhao et al., 2016)
τ_H	0.12 – 0.95 day ⁻¹	0.5294 day ⁻¹	(Stauch et al., 2011; Zhao et al., 2016)
γ_H	0.00556 – 0.01667 day ⁻¹	0.0111 day ⁻¹	(Shimozako et al., 2017)
ψ_V	30 – 70 egg oviposition ⁻¹	50 egg oviposition ⁻¹	(European Centre for Disease Prevention and Control,)
K_M	$9000 - 1.1 \times 10^9$	5.5×10^6	(Hussaini et al., 2016)
μ_E	0.05 – 0.25 day ⁻¹	0.143 day ⁻¹	(European Centre for Disease Prevention and Control,)
μ_L	0.0333 – 0.05 day ⁻¹	0.0455 day ⁻¹	(European Centre for Disease Prevention and Control,)
μ_P	0.0769 – 0.167 day ⁻¹	0.143 day ⁻¹	(European Centre for Disease Prevention and Control,)
μ_M	0.0416 – 0.083 day ⁻¹	0.0714 day ⁻¹	(European Centre for Disease Prevention and Control,)
σ_E	0.05 – 0.25 day ⁻¹	0.0833 day ⁻¹	(European Centre for Disease Prevention and Control,)
σ_L	0.0333 – 0.05 day ⁻¹	0.04 day ⁻¹	(European Centre for Disease Prevention and Control, 2017)
r_L	0.0009 – 0.011 day ⁻¹	0.00893 day ⁻¹	Fitted
σ_P	0.07 – 0.1667 day ⁻¹	0.0833 day ⁻¹	(European Centre for Disease Prevention and Control,)
f	0.413 – 0.9	0.5	Assumed
ξ_L	0.0456 – 0.564 day ⁻¹	0.1 day ⁻¹	(Poché et al., 2016)
ξ_M	0.0192 – 0.469 day ⁻¹	0.0923 day ⁻¹	(Poché et al., 2016)
β_V	0.2 – 0.8	0.7	(Hartemink et al., 2011; Zhao et al., 2016)
Π_R	7.49 – 11.4 day ⁻¹	8.33 day ⁻¹	(The Africa Report, 2013)
μ_R	$1.522 \times 10^{-4} - 5.48 \times 10^{-4}$ day ⁻¹	2.28×10^{-4} day ⁻¹	(PetCareRx, 2013)
b_R	0.03 – 0.2	0.16	(Hartemink et al., 2011; Shimozako et al., 2017)
δ_R	0.0099 – 0.0121 day ⁻¹	0.011 day ⁻¹	(Hartemink et al., 2011)
η_R	1.0 – 1.75	1.39	Fitted
ρ_R	0.00137 – 0.011 day ⁻¹	7.083×10^{-3} day ⁻¹	Fitted
τ_R	0.01 – 0.04 day ⁻¹	0.0233 day ⁻¹	(Hartemink et al., 2011)
γ_R	$3.9 \times 10^{-4} - 0.0167$ day ⁻¹	0.011 day ⁻¹	(Parasites - Leishmaniasis, 2017; Parnell, Guptill, & Solano-Gallego, 2008)

associated parameters ξ_L and ξ_M (for the treatment of infected reservoir hosts) were set to zero, while all other parameters of the model are set at their baseline values in Table 4.

2.1. Basic properties

The basic properties of the model (2.1) will now be explored. It should be noted, first of all, that all parameters of the model are non-negative (with the death rates ($\mu_H, \mu_E, \mu_P, \mu_M, \mu_R$), recruitment rates (Π_H, Π_R), transmission probabilities ($\beta_H, \beta_V, \beta_R$) and the biting rates (b_H, b_V, b_R) assumed to be strictly positive). It is convenient to let $\mu_V = \min\{\mu_E, \mu_L, \mu_P, \mu_M\}$. Consider the following equations for the rate of change of the total human, vector and reservoir host populations:

$$\frac{dN_H}{dt} = \Pi_H - \mu_H N_H - \delta_H I_H \leq \Pi_H - \mu_H N_H, \tag{2.2}$$

$$\begin{aligned} \frac{dN_V}{dt} &= \psi_V \left(1 - \frac{N_{VM}}{K_M}\right) N_{VM} - \xi_M N_{VM} - \xi_L L_V - r_L L_V^2 - (1 - f) \sigma_P P_V - \mu_V N_V \leq \psi_V \left(1 - \frac{N_{VM}}{K_M}\right) N_{VM} - \mu_V N_V \\ &\leq \psi_V K_M - \mu_V N_V, \end{aligned} \tag{2.3}$$

$$\frac{dN_R}{dt} = \Pi_R - \mu_R N_R - \delta_R I_R \leq \Pi_R - \mu_R N_R. \tag{2.4}$$

Furthermore, consider the region:

$$\Omega = \left\{ (S_H, E_H, I_H, R_H, E_V, L_V, P_V, S_V, I_V, S_R, E_R, I_R, T_R) \in \mathbb{R}_+^{13} : N_H(t) \leq \frac{\Pi_H}{\mu_H}, N_V(t) \leq \frac{K_M \psi_V}{\mu_V}, N_R(t) \leq \frac{\Pi_R}{\mu_R} \right\},$$

It can be shown (by solving for $N_H(t), N_V(t)$ and $N_R(t)$ in (2.2), (2.3) and (2.4)) that all solutions of the system starting in the region Ω remain in Ω for all $t \geq 0$. Thus, the region Ω is positively-invariant, and it is sufficient to consider solutions in Ω . In this region, the usual existence, uniqueness and continuation results hold for the system (Forouzannia & Gumel, 2014).

3. Mathematical analysis

3.1. Disease-free equilibria

The model (2.1) has two disease-free equilibria, namely the trivial disease-free equilibrium (TDFE, denoted by \mathcal{T}_0) and a non-trivial disease-free equilibrium (NDFE, denoted by \mathcal{E}_0), as described below.

(i) TDFE (where no sandflies exist):

$$\begin{aligned} \mathcal{T}_0 &= (S_H^*, E_H^*, I_H^*, R_H^*, E_V^*, L_V^*, P_V^*, S_V^*, I_V^*, S_R^*, E_R^*, I_R^*, T_R^*) \\ &= \left(\frac{\Pi_H}{\mu_H}, 0, 0, 0, 0, 0, 0, 0, 0, \frac{\Pi_R}{\mu_R}, 0, 0, 0 \right). \end{aligned}$$

(ii) NDFE:

$$\begin{aligned} \mathcal{E}_0 &= (S_H^\circ, E_H^\circ, I_H^\circ, R_H^\circ, E_V^\circ, L_V^\circ, P_V^\circ, S_V^\circ, I_V^\circ, S_R^\circ, E_R^\circ, I_R^\circ, T_R^\circ) \\ &= \left(\frac{\Pi_H}{\mu_H}, 0, 0, 0, E_V^\circ, L_V^\circ, P_V^\circ, S_V^\circ, 0, \frac{\Pi_R}{\mu_R}, 0, 0, 0 \right), \end{aligned}$$

where,

$$E_V^\circ = \frac{g_L + r_L L_V^\circ}{\sigma_E} L_V^\circ, P_V^\circ = \frac{\sigma_L L_V^\circ}{g_P} S_V^\circ = \frac{\sigma_L f \sigma_P L_V^\circ}{g_P g_M} L_V^\circ, L_V^\circ = \frac{1}{Q} \left(1 - \frac{1}{\mathcal{R}_{EP}} \right),$$

with $Q = \frac{g_E g_P g_M r_L}{\psi_V \sigma_E \sigma_L f \sigma_P} + \frac{\sigma_L f \sigma_P}{g_P g_M K_M}$, $g_E = \sigma_E + \mu_E$, $g_L = \sigma_L + \mu_L + \xi_L$, $g_P = \sigma_P + \mu_P$, $g_M = \mu_M + \xi_M$ and

$$\mathcal{R}_{EP} = \frac{\psi_V \sigma_E \sigma_L f \sigma_P}{(\sigma_E + \mu_E)(\sigma_L + \mu_L + \xi_L)(\sigma_P + \mu_P)(\mu_M + \xi_M)}. \tag{3.1}$$

It follows that the NDFE (\mathcal{E}_0) exists if and only if $\mathcal{R}_{EP} > 1$. Furthermore, the NDFE (\mathcal{E}_0) reduces to the TDFE (\mathcal{T}_0) when $\mathcal{R}_{EP} = 1$. The threshold \mathcal{R}_{EP} is similar to the *vectorsial reproduction number* described in (Okuneye, Abdelrazec, & Gumel, 2018). It measures the average number of new adult female sandflies produced by one reproductive sandfly during its entire reproductive period. It is the product of the eggs oviposition rate (ψ_V), the fraction of eggs that survives and develops into larvae ($\frac{\sigma_E}{\sigma_E + \mu_E}$), the fraction of these larvae that survives and develops into pupae ($\frac{\sigma_L}{\sigma_L + \mu_L + \xi_L}$), the fraction of pupae that survives and develops into female adult sandflies ($\frac{f \sigma_P}{\sigma_P + \mu_P}$) and the average lifespan of adult female sandfly ($\frac{1}{\mu_M + \xi_M}$).

3.1.1. Asymptotic stability of TDFE

Theorem 3.1. *The TDFE of the model (2.1), \mathcal{T}_0 , is globally-asymptotically stable (GAS) in Ω whenever $\mathcal{R}_{EP} \leq 1$.*

Proof. Let $\mathcal{R}_{EP} \leq 1$. Consider, first of all, the sandfly-only system of the model (2.1):

$$\begin{aligned} \frac{dE_V}{dt} &= \psi_V \left(1 - \frac{N_{VM}}{K_M} \right) (S_V + I_V) - (\sigma_E + \mu_E) E_V, \\ \frac{dL_V}{dt} &= \sigma_E E_V - (\sigma_L + \mu_L + \xi_L + r_L L_V) L_V, \\ \frac{dP_V}{dt} &= \sigma_L L_V - (\sigma_P + \mu_P) P_V, \\ \frac{dS_V}{dt} &= \sigma_P f P_V - \lambda_V S_V - (\mu_M + \xi_M) S_V, \\ \frac{dI_V}{dt} &= \lambda_V S_V - (\mu_M + \xi_M) I_V. \end{aligned} \tag{3.2}$$

The system (3.2) has a unique trivial equilibrium (whenever $\mathcal{R}_{EP} \leq 1$), given by

$$\mathcal{T}_{01} = (E_V^*, L_V^*, P_V^*, S_V^*, I_V^*) = (0, 0, 0, 0, 0),$$

in the invariant region

$$\Omega_1 = \left\{ (E_V(t), L_V(t), P_V(t), S_V(t), I_V(t)) \in \mathbb{R}_+^5 : 0 \leq E_V(t), 0 \leq L_V(t), \right. \\ \left. 0 \leq P_V(t), 0 \leq S_V(t), 0 \leq I_V(t), N_V(t) \leq \frac{K_M \psi_V}{\mu_V} \right\},$$

Furthermore, consider the following Lyapunov function for the system (3.2):

$$\mathcal{N}_1 = f \sigma_E \sigma_L \sigma_P E_V + f \sigma_L g_E \sigma_P L_V + f g_E g_L \sigma_P P_V + g_E g_L g_P (S_V + I_V),$$

where, $g_E = \sigma_E + \mu_E, g_L = \sigma_L + \mu_L + \xi_L, g_P = \sigma_P + \mu_P$ and $g_M = \mu_M + \xi_M$, with Lyapunov derivative given by (where a dot represents differentiation with respect to time t):

$$\begin{aligned} \dot{\mathcal{N}}_1 &= \sigma_E \sigma_L \sigma_P f \frac{dE_V}{dt} + \sigma_L g_E \sigma_P f \frac{dL_V}{dt} + g_E g_L \sigma_P f \frac{dP_V}{dt} + g_E g_L g_P \left(\frac{dS_V}{dt} + \frac{dI_V}{dt} \right), \\ &= \sigma_E \sigma_L \sigma_P f \left[\psi_V \left(1 - \frac{N_{VM}}{K_M} \right) (S_V + I_V) - g_E E_V \right] \\ &\quad + \sigma_L g_E \sigma_P f (\sigma_E E_V - g_L L_V) + g_E g_L \sigma_P f (\sigma_L L_V - g_P P_V) + g_E g_L g_P [\sigma_P f P_V - g_M (S_V + I_V)] - \sigma_L g_E \sigma_P f r_L L_V^2, \\ &= \sigma_E \sigma_L \sigma_P f \psi_V \left(1 - \frac{N_{VM}}{K_M} \right) (S_V + I_V) - g_E g_L g_P g_M (S_V + I_V) - \sigma_L g_E \sigma_P f r_L L_V^2, \\ &= g_E g_L g_P g_M \left[(\mathcal{R}_{EP} - 1) - \mathcal{R}_{EP} \frac{N_{VM}}{K_M} \right] (S_V + I_V) - f \sigma_L g_E \sigma_P r_L L_V^2. \end{aligned}$$

Thus, it follows, for $\mathcal{R}_{EP} \leq 1$ in Ω_1 , that the Lyapunov derivative $\dot{\mathcal{N}}_1 < 0$. Furthermore, it follows from the LaSalle's Invariance Principle (Theorem 6.4 of (LaSalle, 1976)) that the maximal invariant set contained in $\{(E_V(t), L_V(t), P_V(t), S_V(t), I_V(t)) \in \Omega_1 : \dot{\mathcal{N}}_1 = 0\}$ is the singleton $\{\mathcal{T}_{01}\}$. Hence, the unique trivial equilibrium (\mathcal{T}_{01}) of the system (3.2) is GAS in Ω_1 whenever $\mathcal{R}_{EP} \leq 1$. Thus, for $\mathcal{R}_{EP} \leq 1$,

$$(E_V(t), L_V(t), P_V(t), S_V(t), I_V(t)) \rightarrow (0, 0, 0, 0, 0), \text{ as } t \rightarrow \infty. \tag{3.3}$$

Since the model (2.1) is Type K (Smith, 1986), it follows, by substituting (3.3) into (2.1), that

$$(S_H, E_H, I_H, R_H, S_R, E_R, I_R, T_R)(t) \rightarrow \left(\frac{\Pi_H}{\mu_H}, 0, 0, 0, \frac{\Pi_R}{\mu_R}, 0, 0, 0 \right), \text{ as } t \rightarrow \infty. \tag{3.4}$$

Thus, by combining Equations (3.3) and (3.4), it follows that the TDFE (\mathcal{T}_0) of the model (2.1) is GAS in Ω whenever $\mathcal{R}_{EP} \leq 1$.

It is worth stating that the trivial equilibrium (\mathcal{T}_0) is ecologically unrealistic, since it is associated with the (unrealistic) scenario where sandflies do not exist.

3.1.2. Asymptotic stability of NDFE

Let $\mathcal{R}_{EP} > 1$ (so that the NDFE, \mathcal{E}_0 , of the model (2.1) exists). It can be shown, using the next generation operator method (Diekmann, Heesterbeek, & Metz, 1990; Van den Driessche & Watmough, 2002), that the associated reproduction number of the model (2.1) (denoted by \mathcal{R}_0) is given by:

$$\mathcal{R}_0 = \sqrt{\mathcal{R}_{VR} \times \mathcal{R}_{RV}}, \tag{3.5}$$

where,

$$\mathcal{R}_{VR} = \frac{b_R \beta_R S_R^0}{g_M (N_H^* + N_R^*)} \tag{3.6}$$

and,

$$\mathcal{R}_{RV} = \frac{b_R \beta_V S_V^\circ}{N_H^* + N_R^*} \left[\frac{\eta_R}{g_1} + \frac{\gamma_R g_3}{g_1 (g_2 g_3 - \tau_R \rho_R)} \right], \tag{3.7}$$

with $N_H^* = \frac{\Pi_H}{\mu_H}$, $N_R^* = \frac{\Pi_R}{\mu_R}$, $g_1 = \gamma_R + \mu_R$, $g_2 = \tau_R + \mu_R + \delta_R$, $g_3 = \rho_R + \mu_R$, $g_M = \mu_M + \xi_M$ and $g_2 g_3 - \tau_R \rho_R = \tau_R \mu_R + (\mu_R + \delta_R) g_3 > 0$. The result below follows from Theorem 2 of (Van den Driessche & Watmough, 2002).

Theorem 3.2. *The NDFE, \mathcal{E}_0 , of the model (2.1), with $\mathcal{R}_{EP} > 1$, is locally-asymptotically stable (LAS) in $\Omega \setminus \{\mathcal{T}_0\}$ if $\mathcal{R}_0 < 1$, and unstable if $\mathcal{R}_0 > 1$.*

The epidemiological implication of Theorem 3.2 is that ZVL can be effectively controlled in the two hosts populations (humans and non-humans animal reservoir hosts) if the initial number infected hosts and vector are small enough (i.e., in the basin of attraction of the non-trivial disease-free equilibrium, \mathcal{E}_0).

Interpretation of \mathcal{R}_0 . The threshold quantity \mathcal{R}_0 is ecologically and epidemiologically interpreted as follows.

1. *Interpretation of \mathcal{R}_{VR} :* The quantity \mathcal{R}_{VR} , given in (3.6), is associated with the infection of susceptible reservoirs by infectious sandflies. It is the product of the infection rate of susceptible reservoirs by infectious sandflies $\left(b_R \beta_{RN} \frac{S_V^\circ}{N_H^* + N_R^*} \right)$ and the average duration of infectious sandflies in the I_V class, $\left(\frac{1}{g_M} \right)$.
2. *Interpretation of \mathcal{R}_{RV} :* The quantity \mathcal{R}_{RV} , given in (3.7), is associated with the infection of susceptible sandflies by exposed (asymptotically infectious) and symptomatically infectious reservoirs. It can further be expressed as

$$\mathcal{R}_{RV} = \mathcal{R}_{E_R V} + \mathcal{R}_{I_R V} + \mathcal{R}_{(I_R \leftrightarrow T_R) V}, \tag{3.8}$$

where,

$$\begin{aligned} \mathcal{R}_{E_R V} &= b_R \beta_V \frac{S_V^\circ}{N_H^* + N_R^*} \cdot \frac{\eta_R}{g_1}, & \mathcal{R}_{I_R V} &= b_R \beta_V \frac{S_V^\circ}{N_H^* + N_R^*} \cdot \frac{\gamma_R}{g_1} \cdot \frac{1}{g_2}, \\ \mathcal{R}_{(I_R \leftrightarrow T_R) V} &= b_R \beta_V \frac{S_V^\circ}{N_H^* + N_R^*} \cdot \frac{\gamma_R}{g_1} \cdot \frac{1}{g_2} \cdot \sum_{i=1}^n \left(\frac{\tau_R \rho_R}{g_2 g_3} \right)^i, \end{aligned}$$

where $n \rightarrow \infty$ is the total number of the cycles at which infectious reservoir received and failed treatment (and returned to the symptomatically-infectious class), $\mathcal{R}_{E_R V}$ accounting for the average number of new infectious sandflies generated by exposed (asymptotically-infectious) reservoirs (E_R), $\mathcal{R}_{I_R V}$ measures the average number of new infectious sandflies generated by symptomatically-infectious reservoirs (I_R) that have not undergone any treatment and $\mathcal{R}_{(I_R \leftrightarrow T_R) V}$ accounts for the average number of new infectious sandflies generated by symptomatically-infectious reservoirs that have undergone (and failed) treatment (and return to the symptomatically-infectious class) at least once. In particular,

- i. $\mathcal{R}_{E_R V}$ is the product of the infection rate of susceptible sandflies by exposed (asymptotically-infected) reservoirs $\left(b_R \beta_V \frac{S_V^\circ}{N_H^* + N_R^*} \right)$, and the average duration in the E_R class, $\left(\frac{1}{g_1} \right)$.
- ii. $\mathcal{R}_{I_R V}$ is the product of the infection rate of susceptible sandflies by symptomatically-infected reservoirs $\left(b_R \beta_V \frac{S_V^\circ}{N_H^* + N_R^*} \right)$, the probability that an exposed reservoir becomes symptomatic (i.e., survived the E_R class and move to the I_R class) $\left(\frac{\gamma_R}{g_1} \right)$, and the average duration in the I_R class, $\left(\frac{1}{g_2} \right)$.
- iii. $\mathcal{R}_{(I_R \leftrightarrow T_R) V}$ is the product of the infection rate of susceptible sandflies by symptomatically infected reservoirs $\mathcal{R}_{I_R V}$ (described above in ii.), and the probability that such infectious reservoirs have received and failed treatment(s) at least once given by $\sum_{i=1}^n \left(\frac{\tau_R \rho_R}{g_2 g_3} \right)^i$ (where $\frac{\tau_R}{g_2}$ is the fraction of symptomatic reservoir hosts who received treatment (and progressed to the T_R class), and $\frac{\rho_R}{g_3}$ is the fraction of reservoir hosts who failed treatment and reverts to the I_R class). It is worth mentioning that the total number of the cycle at which infectious reservoir hosts received and failed treatments (and return to the symptomatically infectious class) is finite (i.e., $n < \infty$). Although ZVL is not completely curable (as

relapses are common when treatment ceases), *euthanasia*¹ is considered in some cases where the animal is chronically infected (and cannot be cured) (Petersen, 2009).

3.2. Backward bifurcation analysis

Backward bifurcation, which has been observed in numerous models for vector-borne diseases (see, for instance (Forouzzannia & Gumel, 2014; Garba, Gumel, & Abu Bakar, 2008)), typically occurs when the asymptotically-stable disease-free equilibrium of the model co-exists with a stable endemic equilibrium when the associated reproduction number (\mathcal{R}_0) of the model is less than unity (Castillo-Chavez & Song, 2004). The epidemiological consequence of backward bifurcation is that having the associated *basic reproduction number* of the model to be less than unity, while necessary, is no longer sufficient for ZVL control (or elimination). In a backward bifurcation situation, effective community-wide control of ZVL (when $\mathcal{R}_0 < 1$) is dependent on the initial sizes of the subpopulations of the model. In other words, backward bifurcation makes effective ZVL control in the community difficult. It is instructive, therefore, to explore the possibility of backward bifurcation in the model (2.1).

Let $\mathcal{E}_1^{**} = (S_H^{**}, E_H^{**}, I_H^{**}, R_H^{**}, E_V^{**}, I_V^{**}, P_V^{**}, S_V^{**}, I_V^{**}, S_R^{**}, E_R^{**}, I_R^{**}, T_R^{**})$ represents an arbitrary non-trivial equilibrium point (EEP) of the model (2.1) and,

$$\lambda_H^{**} = \frac{b_H \beta_H I_V^{**}}{N_H^{**} + N_R^{**}}, \lambda_V^{**} = \frac{b_R \beta_V (\eta_R E_R^{**} + I_R^{**})}{N_H^{**} + N_R^{**}}, \lambda_R^{**} = \frac{b_R \beta_R I_V^{**}}{N_H^{**} + N_R^{**}}.$$

Solving the equations of the model (2.1) at \mathcal{E}_1^{**} gives:

$$\begin{aligned} S_H^{**} &= \frac{\Pi_H}{\lambda_H^{**} + \mu_H}, E_H^{**} = \frac{\lambda_H^{**}}{g_4} S_H^{**}, I_H^{**} = \frac{\gamma_H E_H^{**}}{g_5}, R_H^{**} = \frac{\tau_H I_H^{**}}{\mu_H}, \\ E_V^{**} &= \frac{\psi_V \sigma_L \sigma_P}{G^2} (\mathcal{R}_{EP} - 1), I_V^{**} = \frac{g_P g_M K_M}{G} (\mathcal{R}_{EP} - 1), P_V^{**} = \frac{\sigma_L L_V^{**}}{g_P}, \\ S_V^{**} &= \frac{f \sigma_P}{\lambda_V^{**} + g_M} P_V^{**}, I_V^{**} = \frac{\lambda_V^{**}}{g_M} S_V^{**}, S_R^{**} = \frac{\Pi_R}{\lambda_R^{**} + \mu_R}, E_R^{**} = \frac{\lambda_R^{**}}{g_1} S_R^{**}, \\ I_R^{**} &= \frac{g_3 \gamma_R}{g_2 g_3 - \rho_R \tau_R} E_R^{**}, T_R^{**} = \frac{\tau_R I_R^{**}}{g_3}, \end{aligned} \tag{3.9}$$

where

$$G = f^2 \psi_V \sigma_E \sigma_L^2 \sigma_P^2 + K_M g_3 g_5^2 g_M^2 r_L, g_1 = \gamma_R + \mu_R, g_2 = \tau_R + \mu_R + \delta_R, g_3 = \rho_R + \mu_R, g_4 = \gamma_H + \mu_H, g_5 = \tau_H + \mu_H, g_E = \sigma_E + \mu_E, g_L = \sigma_L + \mu_L + \xi_L, g_P = \sigma_P + \mu_P, g_M = \mu_M + \xi_M, N_{VM}^{**} = S_V^{**} + I_V^{**} \text{ and } \mathcal{R}_{EP} \text{ is as given in Equation (3.1).}$$

For mathematical tractability, the computations will be carried out for the special case of the model (2.1) in the absence of disease-induced mortality in humans (i.e., $\delta_H = 0$) and larval density-dependence (i.e., $r_L = 0$). Let $\mathcal{R}_1 = \mathcal{R}_0|_{\delta_H=r_L=0}$. It can be shown, by solving for the variables of the resulting reduced version of the model (2.1) at steady-state and $\delta_H = r_L = 0$ (and simplifying), that the solutions of the resulting model (at steady-state, \mathcal{E}_1^{**}) satisfy the following quadratic (in terms of λ_R^{**}):

$$A_0 (\lambda_R^{**})^2 + A_1 (\lambda_R^{**}) + A_2 = 0, \tag{3.10}$$

where,

$$\begin{aligned} A_0 &= g_E g_L g_P g_M \mathcal{R}_{EP} D_1 [g_M D_1 + b_R \beta_V \Pi_R \eta_R (g_2 g_3 - \tau_R \rho_R) + b_R \beta_V \Pi_R g_3 \gamma_R], \\ A_1 &= g_E g_L g_P g_M^2 g_1^2 \mu_R (g_2 g_3 - \tau_R \rho_R)^2 (N_H^* + N_R^*) \mathcal{R}_{EP} \left\{ 2 \frac{D_1}{D_2} - (N_H^* + N_R^* - b_R S_R^* S_V^*) \mathcal{R}_1^2 \right\}, \\ A_2 &= g_E g_L g_P g_M^2 g_1 (\tau_R \mu_R + (\mu_R + \delta_R) g_3) (N_H^* + N_R^*)^2 \mathcal{R}_{EP} (1 - \mathcal{R}_1^2), \end{aligned}$$

with,

$$D_1 = (g_1 N_H^* + \Pi_R) (g_2 g_3 - \tau_R \rho_R) + \Pi_R \gamma_R (g_3 + \tau_R) \text{ and } D_2 = g_M g_1 (g_2 g_3 - \tau_R \rho_R).$$

The results below follows from Equation (3.10).

Theorem 3.3. Let $\mathcal{R}_{EP} > 1$. The model (2.1) with $\delta_H = r_L = 0$ has:

¹ Euthanasia is the painless killing of a patient suffering from an incurable and painful disease.

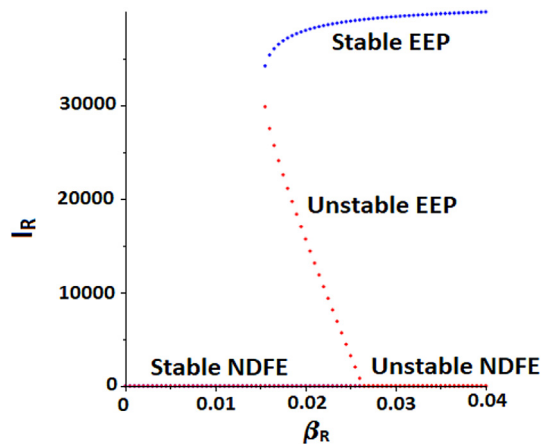


Fig. 4. Backward bifurcation diagrams of the model (2.1) in the absence of disease-induced death in humans (i.e., $\delta_H = 0$). Parameter values used are as given by their baseline values in Table 4 with $\Pi_R = 500$.

- (i) a unique endemic equilibrium if $A_2 < 0 \Leftrightarrow \mathcal{R}_1 > 1$;
- (ii) a unique endemic equilibrium if $A_1 < 0$, and $A_2 = 0$ or $A_1^2 - 4A_0A_2 = 0$;
- (iii) two endemic equilibria if $A_2 > 0$ ($\mathcal{R}_1 < 1$), $A_1 < 0$ and $A_1^2 - 4A_0A_2 > 0$;
- (iv) no endemic equilibrium otherwise.

Item (iii) of Theorem 3.3 suggests the possibility of a backward bifurcation in the model (2.1) (since the model could have two endemic equilibria when $\mathcal{R}_1 < 1$). This is explored below.

Theorem 3.4. The special case of the model (2.1) with $\delta_H = r_L = 0$ undergoes a backward bifurcation at $\mathcal{R}_1 = 1$ whenever the inequality (A-3), given in Appendix A, holds.

The proof of Theorem 3.4, based on using Centre Manifold theory (Castillo-Chavez & Song, 2004; Forouzannia & Gumel, 2014), is given in Appendix A. Fig. 4 depicts the backward bifurcation diagram of model (2.1) for the cases with $\delta_H = 0$ (Fig. 4(a)), $\delta_R = 0$ (Fig. 4(b)) and $\delta_H \neq 0$ and $\delta_R \neq 0$ (Fig. 4(c)).

It is worth mentioning that, for a special case of the model with negligible disease-induced mortality in the host populations (such as $\delta_H = \delta_R = 0$), the expressions for the backward bifurcation coefficients a and b given by Equations (A-2) and (A-3), respectively, in Appendix A, reduce to (it should be noted from Appendix A that eigenvectors v_9, v_{11} and w_9 are all positive, while w_8 and w_{10} are negative):

$$a = -2w_8w_{10} \left(\frac{g_M}{S_R^0} v_9 + \frac{\mu_R}{S_V^0} v_{11} \right) < 0 \text{ and } b = b_R v_{11} w_9 > 0.$$

Hence, it follows from Theorem 4.1 in (Castillo-Chavez & Song, 2004), that the special case of the model (2.1) with $\delta_H = \delta_R = 0$ will not undergo a backward bifurcation at $\mathcal{R}_2 = \mathcal{R}_0|_{\delta_H=\delta_R=0} = 1$. This result is consistent with those reported for the dynamics of vector borne diseases, such as those in (Bowman et al., 2005; Forouzannia & Gumel, 2014; Garba et al., 2008; Hussaini et al., 2016). The global asymptotic stability of the non-trivial equilibrium (\mathcal{E}_0) of the model (2.1) is proved below for the aforementioned special case.

Theorem 3.5. The NDFE, \mathcal{E}_0 , of the special case of the model (2.1) with $\delta_H = \delta_R = 0$ is GAS in $\Omega \setminus \{\mathcal{F}_0\}$ whenever $\mathcal{R}_{EP} > 1$ and $\mathcal{R}_2 = \mathcal{R}_0|_{\delta_H=\delta_R=0} < 1$.

The proof, based on the approach in (Dumont & Chiroleu, 2010; Okuneye & Gumel, 2017), is given in Appendix B. The epidemiological implication of Theorem 3.5 is that, for the special case of the model (2.1) with negligible disease-induced mortality in the host populations (i.e., $\delta_H = \delta_R = 0$), bringing (and maintaining) the threshold quantity \mathcal{R}_2 to a value less than unity is necessary and sufficient for the effective control (or elimination) of ZVL in the human and animal reservoir populations.

4. Sensitivity analysis and numerical simulations

The model (2.1) contains 30 parameters, and uncertainties in the estimates of these parameters are expected to arise. The effect of such uncertainties is assessed using Latin Hypercube Sampling (LHS) (Blower & Dowlatabadi, 1994; Marino, Hogue, Ray, & Kirschner, 2008; McLeod, Brewster, Gumel, & Slonowsky, 2006; Mckay, Beckman, & Conover, 1979). Furthermore,

Table 5

PRCC values for the parameters of the model (2.1) using the basic reproduction number (\mathcal{R}_0) as response function (the top three (most dominant) parameters that affect the dynamics of the model with respect to \mathcal{R}_0 are highlighted in bold font). Parameter values and ranges used are as given in Table 4.

Parameters	PRCC $_{\mathcal{R}_0}$	Parameters	PRCC $_{\mathcal{R}_0}$	Parameters	PRCC $_{\mathcal{R}_0}$
Π_H	-0.15	ρ_R	+0.016	σ_P	+0.36
μ_H	+0.14	δ_R	-0.049	μ_P	-0.31
Π_R	+0.053	ψ_V	+0.42	f	+0.39
μ_R	-0.23	σ_E	+0.35	β_V	+0.37
η_R	+0.14	μ_E	-0.36	μ_{MT}	-0.91
b_R	+0.74	σ_L	+0.33	r_L	-0.061
β_R	+0.38	μ_{LT}	-0.28	K_M	-0.0016
γ_R	-0.51	τ_R	-0.0047		

sensitivity analysis (using Partial Rank Correlation Coefficients (PRCC)) is carried out to determine the parameters that have the greatest influence on the dynamics of the disease (using the basic reproduction number (\mathcal{R}_0) as response function (as shown in Table 5)). The ranges and baseline values of the parameters tabulated in Table 4 will be used in this analysis.

The top three PRCC-ranked parameters are the sandfly removal rate (given by the aggregated parameter μ_{MT} , defined as $\mu_{MT} = \mu_M + \xi_M$), the biting rate of sandflies on reservoir hosts (b_R), the progression rate of exposed reservoirs to active ZVL class (γ_R). Furthermore, parameters such as the sandfly oviposition rate (ψ_V), fraction of female sandfly reaching adult stage (f), probabilities of infection per bite (β_R, β_V), progression rate of immature sandfly ($\sigma_i, i = E, L, P$), death rates of immature sandfly ($\mu_i, i = E, L, P$) are also influential (but not as dominant as the aforementioned top three PRCC-ranked parameters). Thus, this study shows that effective disease control entails a multi-faceted approach based on minimizing the contact reservoirs have with sandflies (i.e., minimizing b_R and β_R by clearing sandfly breeding sites around the reservoirs and spraying of sandfly repellents), reducing sandfly population (i.e., increasing μ_{MT} ($i = MT, E, L, P$) and reducing σ_i ($i = E, L, P$) by clearing sandfly breeding sites around the reservoirs) and early diagnosis of ZVL cases in reservoirs (i.e., increasing γ_R by ZVL screening to high-risk individuals).

The effect of the average lifespan (survival) of sandflies ($1/\mu_{MT}$) and animal reservoir hosts ($1/\mu_R$) is monitored by simulating the model (2.1) using the baseline parameter values in Table 4 (relevant to ZVL dynamics in Aracatuba municipality, Brazil (Shimozako et al., 2017)). A contour plot of \mathcal{R}_0 , as a function of $1/\mu_{MT}$ and $1/\mu_R$, shows that \mathcal{R}_0 (i.e., disease burden) increases with increasing survival of both the vector ($1/\mu_{MT}$) and animal reservoir hosts ($1/\mu_R$), as expected (Fig. 5). In particular, the range of \mathcal{R}_0 values now increases to $\mathcal{R}_0 \in [0.3, 1.4]$, with a mean of $\mathcal{R}_0 = 0.85$. It should be noted that these simulations were generated for the case when $\xi_L = \xi_M = 0$ (since insecticide-based treatment strategy of the reservoir hosts was not implemented in the Aracatuba municipality during the 1999–2015 study period). However, in the hypothetical scenario where such treatment is used (and at the baseline rates given in Table 4), the range of \mathcal{R}_0 significantly decreases to $\mathcal{R}_0 \in [0.1, 0.6]$, with a mean of $\mathcal{R}_0 = 0.35$ (Fig. 6). This represents about 60% reduction in the mean value of \mathcal{R}_0 . Although the default scenario also suggests the feasibility of effective disease control (since the mean value of \mathcal{R}_0 is $\mathcal{R}_0 = 0.85 < 1$; and Theorem 3.5 shows that disease elimination is feasible, if δ_H and δ_R are small enough and $\mathcal{R}_0 < 1$), the latter (hypothetical) scenario, where infected reservoirs are treated, significantly enhances the prospect of disease elimination in the municipality (since the mean value of \mathcal{R}_0 is 0.35). This is quite intuitive, since the population of sandflies obviously decreases if the larvae and adult sandflies continue to feed from the faeces of infected reservoirs. But this poses an ecological dilemma, since treatment of reservoirs can lead to perhaps the removal of sandflies from the local ecosystem (albeit it serves a major

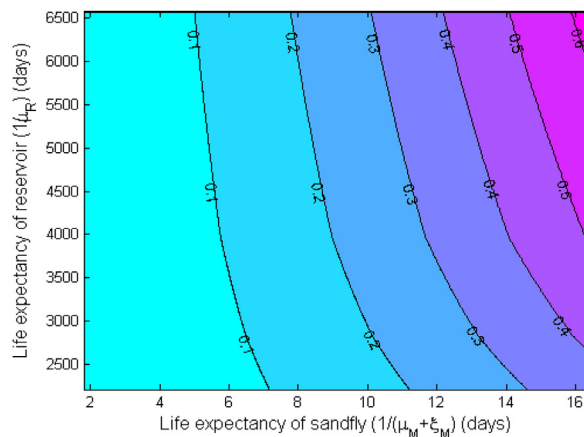


Fig. 5. Contour plot of \mathcal{R}_0 , as a function of the average life expectancy of sandflies ($1/(\mu_M + \xi_M)$) and animal reservoir hosts ($1/\mu_R$). Parameter values used are as in Table 4.

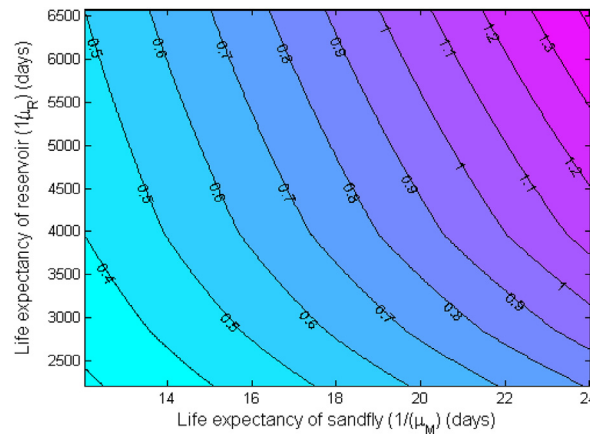


Fig. 6. Contour plot of \mathcal{R}_0 , as a function of the average life expectancy of sandflies ($1/\mu_M$) and animal reservoirs ($1/\mu_R$). Parameter values used are as in Table 4.

epidemiological function of minimizing, or even eliminating, ZVL burden in the community). These simulations show that ZVL modeling studies in communities where such insecticide-based treatment strategy of infected reservoirs is implemented may well be over-estimating the disease burden if they failed to explicitly incorporate the effect of such treatment (i.e., additional larval and adult sandfly mortality due to their feeding on the faeces of the treated infected reservoirs) in the model. Fig. 5 further shows that \mathcal{R}_0 is more sensitive to increases in sandfly lifespan than that of the animal reservoir (so, a strategy that focuses on reducing sandflies, rather than the animal reservoir (e.g., via culling), may be more effective in reducing ZVL burden in the community).

Conclusions

This study is based on the design, analysis and numerical simulations of a new deterministic model for assessing the transmission dynamics of zoonotic visceral leishmaniasis (ZVL) in a community. The model is fitted using case and demographic data relevant to ZVL dynamics in Aracatuba municipality in Brazil. The main theoretical and epidemiological findings of the study are summarized below.

- (i) The model has a trivial disease-free equilibrium (TDFE) which is globally-asymptotically stable if a certain vectorial threshold quantity (\mathcal{R}_{EP}) is less than unity. It also has a non-trivial disease-free equilibrium (NDFE; whenever \mathcal{R}_{EP} is greater than unity) which undergoes a backward bifurcation under certain conditions. In the absence of backward bifurcation, the NDFE is globally-asymptotically stable, for a special case whenever the associated reproduction number is less than unity.
- (ii) Sensitivity analysis of the model (using the *basic reproduction number* (\mathcal{R}_0) as the response function) show that the top three PRCC-ranked parameters are the sandfly removal rate ($\mu_{MT} = \mu_M$ and ξ_M), the biting rate of sandflies on reservoir hosts (b_R), the progression rate of exposed reservoirs to active ZVL class (γ_R). Hence, this study identifies the parameters that should be targeted for effective anti-ZVL control in the community. Other parameters with high PRCC ranking (but not as high as the aforementioned three) are sandfly oviposition rate (ψ_V), the fraction of pupae that became adult female sandflies (f), and the infection probabilities β_R and β_V .
- (iii) Numerical simulations, using the data for ZVL dynamics in Aracatuba municipality during the 1999–2015 study period, show that the associated reproduction number (\mathcal{R}_0) ranges from 0.3 to 1.4, with a mean of 0.85. This range dramatically decreases, to $\mathcal{R}_0 \in [0.1, 0.6]$ (with a mean of 0.35), when insecticide-based treatment of the animal reservoir hosts is implemented. Thus, the prospect of the effective control of ZVL in the community is greatly enhanced if a control strategy based on using insecticide-based treatment of the animal reservoir is implemented. Furthermore, ZVL modeling studies in communities where such treatment is used may be over-estimating the disease burden if they fail to explicitly incorporate the effect of such treatment (i.e., resulting in additional larval and adult sandfly mortality) in the model formulation.
- (iv) The reproduction number \mathcal{R}_0 is more sensitive to increases in sandfly lifespan than that of the animal reservoir (so, a strategy that focuses on reducing sandflies, rather than the animal reservoir (e.g., via culling), may be more effective in reducing ZVL burden in the community).

Appendix A. Proof of Theorem 3.4

Proof. To apply this theory, it is convenient to let $x_1 = S_H, x_2 = E_H, x_3 = I_H, x_4 = R_H, x_5 = E_V, x_6 = L_V, x_7 = P_V, x_8 = S_V, x_9 = I_V, x_{10} = S_R, x_{11} = E_H, x_{12} = I_H$ and $x_{13} = R_H$. Furthermore, let $f = [f_1, \dots, f_{13}]$ denote the vector field of the model (2.1). Then the model (2.1) can be re-written as

$$\begin{aligned}
 \frac{dx_1}{dt} &= f_1 = \Pi_H - \frac{b_H \beta_H x_9}{N_H + N_R} x_1 - \mu_H x_1, \\
 \frac{dx_2}{dt} &= f_2 = \frac{b_H \beta_H x_9}{N_H + N_R} x_1 - (\gamma_H + \mu_H) x_2, \\
 \frac{dx_3}{dt} &= f_3 = \gamma_H x_2 - (\tau_H + \mu_H + \delta_H) x_3, \\
 \frac{dx_4}{dt} &= f_4 = \tau_H x_3 - \mu_H x_4, \\
 \frac{dx_5}{dt} &= f_5 = \psi_V \left(1 - \frac{x_8 + x_9}{K_M} \right) (x_8 + x_9) - (\sigma_E + \mu_E) x_5, \\
 \frac{dx_6}{dt} &= f_6 = \sigma_E x_5 - (\sigma_L + \mu_L + \xi_L + r_L L_V) x_6, \\
 \frac{dx_7}{dt} &= f_7 = \sigma_L x_6 - (\sigma_P + \mu_P) x_7, \\
 \frac{dx_8}{dt} &= f_8 = \sigma_P f x_7 - \frac{b_R \beta_V (\eta_R x_{11} + x_{12})}{N_H + N_R} x_8 - (\mu_M + \xi_M) x_8, \\
 \frac{dx_9}{dt} &= f_9 = \frac{b_R \beta_V (\eta_R x_{11} + x_{12})}{N_H + N_R} x_8 - (\mu_M + \xi_M) x_9, \\
 \frac{dx_{10}}{dt} &= f_{10} = \Pi_R - \frac{b_R \beta_R x_9}{N_H + N_R} x_{10} - \mu_R x_{10}, \\
 \frac{dx_{11}}{dt} &= f_{11} = \frac{b_R \beta_R x_9}{N_H + N_R} x_{10} - (\gamma_R + \mu_R) x_{11}, \\
 \frac{dx_{12}}{dt} &= f_{12} = \gamma_R x_{11} + \rho_R x_{13} - (\tau_R + \mu_R + \delta_R) x_{12}, \\
 \frac{dx_{13}}{dt} &= f_{13} = \tau_R x_{12} - (\rho_R + \mu_R) x_{13}.
 \end{aligned} \tag{A-1}$$

The Jacobian of the transformed model (A-1), evaluated at the non-trivial equilibrium point (\mathcal{E}_0), is given by

$$J(\mathcal{E}_0) = \begin{bmatrix} \mathbf{A} & \mathbf{B} \\ \mathbf{0} & \mathbf{C} \end{bmatrix}$$

where,

$$\mathbf{A} = \begin{bmatrix} -\mu_H & 0 & 0 & 0 & 0 & 0 & 0 & 0 \\ 0 & -g_4 & 0 & 0 & 0 & 0 & 0 & 0 \\ 0 & \gamma_H & -g_5 & 0 & 0 & 0 & 0 & 0 \\ 0 & 0 & \tau_H & -\mu_H & 0 & 0 & 0 & 0 \\ 0 & 0 & 0 & 0 & -g_E & 0 & 0 & \psi_V \left(1 - \frac{2S_V^0}{K_M} \right) \\ 0 & 0 & 0 & 0 & \sigma_E & -g_L & 0 & 0 \\ 0 & 0 & 0 & 0 & 0 & \sigma_L & -g_P & 0 \\ 0 & 0 & 0 & 0 & 0 & 0 & f \sigma_P & -g_M \end{bmatrix},$$

$$\mathbf{B} = \begin{bmatrix} \frac{\beta_H b_H^0 S_H^{\circ}}{S_H^{\circ} + S_R^{\circ}} & 0 & 0 & 0 & 0 & 0 \\ \frac{\beta_H b_H^0 S_H^{\circ}}{S_H^{\circ} + S_R^{\circ}} & 0 & 0 & 0 & 0 & 0 \\ 0 & 0 & 0 & 0 & 0 & 0 \\ 0 & 0 & 0 & 0 & 0 & 0 \\ \psi_V \left(1 - \frac{2S_V^{\circ}}{K_M} \right) & 0 & 0 & 0 & 0 & 0 \\ 0 & 0 & 0 & 0 & 0 & 0 \\ 0 & 0 & 0 & 0 & 0 & 0 \\ 0 & 0 & \frac{\beta_V b_R \eta_R S_V^{\circ}}{S_H^{\circ} + S_R^{\circ}} & \frac{\beta_V b_R S_V^{\circ}}{S_H^{\circ} + S_R^{\circ}} & 0 & 0 \end{bmatrix},$$

$$\mathbf{C} = \begin{bmatrix} 0 & 0 & \frac{\beta_V b_R \eta_R S_V^{\circ}}{S_H^{\circ} + S_R^{\circ}} & \frac{\beta_V b_R S_V^{\circ}}{S_H^{\circ} + S_R^{\circ}} & 0 \\ \frac{\beta_R b_R S_R^{\circ}}{S_H^{\circ} + S_R^{\circ}} & 0 & 0 & 0 & 0 \\ \frac{\beta_R b_R S_R^{\circ}}{S_H^{\circ} + S_R^{\circ}} & 0 & -g_1 & 0 & 0 \\ 0 & 0 & \gamma_R & -g_2 & \rho_R \\ 0 & 0 & 0 & \tau_R & -g_3 \end{bmatrix},$$

with $g_1 = \gamma_R + \mu_R$, $g_2 = \tau_R + \mu_R + \delta_R$, $g_3 = \rho_R + \mu_R$, $g_4 = \gamma_H + \mu_H$, $g_5 = \tau_H + \mu_H + \delta_H$, $g_E = \sigma_E + \mu_E$, $g_L = \sigma_L + \mu_L + \xi_L$, $g_P = \sigma_P + \mu_P$ and $\mathbf{0}$ is a 5×8 zero matrix. Consider the case of the model (2.1) (with $\delta_H = r_L = 0$) when $\mathcal{R}_1 = 1$. Suppose, further $\beta_R = \beta_R^*$ is chosen as a bifurcation parameter. Solving for β_R from $\mathcal{R}_1 = 1$ gives

$$\beta_R = \beta_R^* = \frac{g_1 g_M (N_H^* + N_R^*)^2 (g_2 g_3 - \tau_R \rho_R)}{(b_R)^2 \beta_V S_V^{\circ} S_R^{\circ} [\eta_R (g_2 g_3 - \tau_R \rho_R) + \gamma_R g_3]}.$$

The right eigenvector of $J(\mathcal{E}_0)|_{\beta_R = \beta_R^*}$ is given by $\mathbf{w} = (w_1, w_2, w_3, w_4, w_5, w_6, w_7, w_8, w_9, w_{10}, w_{11}, w_{12}, w_{13})$, where,

$$w_1 = -\frac{\beta_H b_H^0 g_1 S_H^{\circ} w_{11}}{\mu_H b_R \beta_R^* S_R^{\circ}} < 0, w_2 = \frac{\mu_H w_1}{g_4} > 0, w_3 = \frac{\gamma_H w_2}{g_5} > 0, w_4 = \frac{\tau_H w_3}{\mu_H} > 0,$$

$$w_5 = w_6 = w_7 = 0, w_8 = -\frac{\mu_H (S_H^{\circ} + S_R^{\circ}) w_1}{\beta_H b_H^0 S_H^{\circ}} > 0, w_9 = -w_8 < 0, w_{10} = -\frac{g_1 \beta_R w_{11}}{\beta_R^* \mu_R} < 0,$$

$$w_{11} = w_{11} > 0, w_{12} = \frac{\gamma_R g_3 w_{11}}{g_2 g_3 - \tau_R \rho_R} > 0, w_{13} = \frac{\tau_R w_{12}}{g_3} > 0.$$

Similarly, $J(\mathcal{E}_0)|_{\beta_R = \beta_R^*}$ has a left eigenvector $\mathbf{v} = (v_1, v_2, v_3, v_4, v_5, v_6, v_7, v_8, v_9, v_{10}, v_{11}, v_{12}, v_{13})$, where

$$v_1 = v_2 = \dots = v_8 = v_{10} = 0, v_9 = \frac{\beta_R b_R^0 S_R^{\circ} v_{11}}{g_M (S_H^{\circ} + S_R^{\circ})} > 0, v_{11} = v_{11} > 0,$$

$$v_{12} = \frac{\beta_V b_R \rho_R S_V^{\circ} v_9}{(S_H^{\circ} + S_R^{\circ}) (g_2 g_3 - \tau_R \rho_R)} > 0, v_{13} = \frac{\rho_R v_{12}}{g_3} > 0.$$

The eigenvectors v_{11} and w_{11} are chosen so that $\mathbf{v} \cdot \mathbf{w} = 1$ (in line with (Castillo-Chavez & Song, 2004)).

The transformed model (A-1), with $\beta_R = \beta_R^*$, has a simple eigenvalue with zero real part (and all other eigenvalues have negative real part). Hence, the Centre Manifold theory (Carr, 1981; Castillo-Chavez & Song, 2004; Van den Driessche & Watmough, 2002) can be used to analyze the dynamics of the model (A-1) near $\beta_R = \beta_R^*$ (Carr, 1981). In particular, Theorem 4.1 in (Castillo-Chavez & Song, 2004) will be used. It can be shown, by computing the non-zero partial derivatives of the right-

hand side functions, f_i ($i = 1, \dots, 13$, that the associated backward bifurcation coefficients, denoted by a_1 and b_1 (for all parameters ϕ of model (2.1)), are given, respectively, by (see Theorem 4.1 in (Castillo-Chavez & Song, 2004)):

$$\begin{aligned}
 a_1 &= \sum_{k,i,j=1}^{13} v_k w_i w_j \frac{\partial^2 f_k}{\partial x_i \partial x_j}(0, 0) \\
 &= \frac{2M_1 v_{13} w_{11}}{S_H^\circ + S_R^\circ} [(g_2 g_3 - \tau_R \rho_R)(M_2 - M_3) - 2w_{11} M_4] + M_5,
 \end{aligned}
 \tag{A-2}$$

where,

$$\begin{aligned}
 M_1 &= \eta_R (g_2 g_3 - \tau_R \rho_R) + g_3 \gamma_R > 0, M_2 = w_3 - w_{10} > 0, \\
 M_3 &= \frac{\eta_R [(S_H^\circ)^2 + (S_R^\circ)^2] w_{11} g_M M_1 + w_9 w_{12} S_H^\circ S_R^\circ}{S_V^\circ (S_H^\circ + S_R^\circ)} > 0, \\
 M_4 &= \frac{(S_H^\circ + S_R^\circ)^2 + 2S_H^\circ S_R^\circ}{(S_H^\circ + S_R^\circ)^2} + \frac{\gamma_R (S_H^\circ + S_R^\circ) S_H^\circ + \gamma_H (S_H^\circ)^2}{g_M (S_H^\circ + S_R^\circ)^2 (g_2 g_3 - \tau_R \rho_R)} > 0, \\
 M_5 &= \frac{2\eta_R w_{10} w_{11} v_{13}}{(S_H^\circ + S_R^\circ) S_V^\circ S_R^\circ} < 0,
 \end{aligned}$$

and,

$$b_1 = \sum_{k,i=1}^{13} v_k w_i \frac{\partial^2 f_k}{\partial x_i \partial \beta_R^*}(0, 0) = \frac{g_1}{\beta_R^*} v_{11} w_{11} > 0.$$

It follows from (A-2) that the bifurcation coefficient, a , is positive whenever,

$$2M_1 M_2 v_{13} w_{11} (g_2 g_3 - \tau_R \rho_R) > 2M_1 v_{13} w_{11} [(g_2 g_3 - \tau_R \rho_R) M_3 + 2w_{11} M_4] - M_5 (S_H^\circ + S_R^\circ).
 \tag{A-3}$$

Thus, it follows from Theorem 4.1 of (Castillo-Chavez & Song, 2004) that the model (2.1) undergoes a backward bifurcation at $\mathcal{R}_1 = 1$ whenever Inequality (A-3) holds.

Appendix B. Proof of Theorem 3.5

Proof. Consider the special case of the model (2.1) with $\delta_H = \delta_R = 0$ so that $N_H(t) \rightarrow N_H^* = \frac{\Pi_H}{\mu_H}$ and $N_R(t) \rightarrow N_R^* = \frac{\Pi_R}{\mu_R}$, as $t \rightarrow \infty$. Furthermore, let $\mathcal{R}_{EP} > 1$ (so that \mathcal{E}_0 exists) and $\mathcal{R}_2 < 1$. Define $x = (S_H(t), R_H(t), E_V(t), L_V(t), P_V(t), S_V(t), S_R(t), 0, 0, E_H(t), I_H(t), 0, 0, 0, I_V(t), E_R(t), I_R(t), T_R(t))$. Following (Dumont & Chiroleu, 2010; Okuneye & Gumel, 2017), it is convenient to re-write the model (2.1) (without the compartments for individuals with prior immunity and the sandfly compartments) in the following form:

$$\begin{aligned}
 \frac{dx_S}{dt} &= A_1(x)(x_S - x_{NDFE,S}) + A_{12}(x)x_I, \\
 \frac{dx_I}{dt} &= A_2(x)x_I,
 \end{aligned}
 \tag{B-1}$$

where,

$$\begin{aligned}
 x_S(t) &= (S_H(t), R_H(t), E_V(t), L_V(t), P_V(t), S_V(t), S_R(t), 0, 0)^T, \\
 x_I(t) &= (E_H(t), I_H(t), 0, 0, 0, I_V(t), E_R(t), I_R(t), T_R(t))^T, \\
 x_{NDFE,S} &= (S_H^\circ, 0, E_V^\circ, L_V^\circ, P_V^\circ, S_V^\circ, S_R^\circ, 0, 0)^T,
 \end{aligned}$$

with,

$$A_1(x) = \begin{bmatrix} -\mu_H & 0 & 0 & 0 & 0 & 0 & 0 & 0 & 0 \\ 0 & -\mu_H & 0 & 0 & 0 & 0 & 0 & 0 & 0 \\ 0 & 0 & -(\sigma_E + \mu_E) & 0 & 0 & \psi_V \left(1 - \frac{S_V + S_V^s}{K_M}\right) & 0 & 0 & 0 \\ 0 & 0 & \sigma_E & -(\sigma_L + \mu_L + \xi_L) - r_L L_V & 0 & 0 & 0 & 0 & 0 \\ 0 & 0 & 0 & \sigma_L & -(\sigma_P + \mu_P) & 0 & 0 & 0 & 0 \\ 0 & 0 & 0 & 0 & f\sigma_P & -(\mu_M + \xi_M) & 0 & 0 & 0 \\ 0 & 0 & 0 & 0 & 0 & 0 & -\mu_R & 0 & 0 \\ 0 & 0 & 0 & 0 & 0 & 0 & 0 & 0 & 0 \\ 0 & 0 & 0 & 0 & 0 & 0 & 0 & 0 & 0 \end{bmatrix},$$

$$A_{12}(x) = \begin{bmatrix} 0 & 0 & 0 & 0 & 0 & \frac{-b_H \beta_H S_H}{N_H^* + N_R^*} & 0 & 0 & 0 \\ 0 & \tau_H & 0 & 0 & 0 & 0 & 0 & 0 & 0 \\ 0 & 0 & 0 & 0 & 0 & 0 & \psi_V \frac{S_V}{K_M} & 0 & 0 \\ 0 & 0 & 0 & 0 & 0 & 0 & 0 & 0 & 0 \\ 0 & 0 & 0 & 0 & 0 & 0 & 0 & 0 & 0 \\ 0 & 0 & 0 & 0 & 0 & 0 & \frac{-b_R \beta_V \eta_R S_V}{N_H^* + N_R^*} & \frac{-b_R \beta_V S_V}{N_H^* + N_R^*} & 0 \\ 0 & 0 & 0 & 0 & 0 & \frac{-b_R \beta_R S_R}{N_H^* + N_R^*} & 0 & 0 & 0 \\ 0 & 0 & 0 & 0 & 0 & 0 & 0 & 0 & 0 \\ 0 & 0 & 0 & 0 & 0 & 0 & 0 & 0 & 0 \end{bmatrix},$$

and,

$$A_2(x) = \begin{bmatrix} -(\gamma_H + \mu_H) & 0 & 0 & 0 & 0 & \frac{b_H \beta_H S_H}{N_H^* + N_R^*} & 0 & 0 & 0 \\ \gamma_H & -(\tau_H + \mu_H) & 0 & 0 & 0 & 0 & 0 & 0 & 0 \\ 0 & 0 & 0 & 0 & 0 & 0 & 0 & 0 & 0 \\ 0 & 0 & 0 & 0 & 0 & 0 & 0 & 0 & 0 \\ 0 & 0 & 0 & 0 & 0 & 0 & 0 & 0 & 0 \\ 0 & 0 & 0 & 0 & 0 & -(\mu_M + \xi_M) & \frac{b_R \beta_V \eta_R S_V}{N_H^* + N_R^*} & \frac{b_R \beta_V S_V}{N_H^* + N_R^*} & 0 \\ 0 & 0 & 0 & 0 & 0 & \frac{b_R \beta_R S_R}{N_H^* + N_R^*} & -(\gamma_R + \mu_R) & 0 & 0 \\ 0 & 0 & 0 & 0 & 0 & 0 & \gamma_R & -(\tau_R + \mu_R) & \rho_R \\ 0 & 0 & 0 & 0 & 0 & 0 & 0 & \tau_R & -(\rho_R + \mu_R) \end{bmatrix},$$

It can be verified that the eigenvalues of $A_1(x)$ are real and non-positive. Hence, the system $\frac{dx_S}{dt} = A_1(x)(x_S - x_{NDFE,S})$ is GAS at $x_{NDFE,S}$ (Dumont & Chiroleu, 2010). It should be noted that the matrix $A_2(x)$ is a Metzler irreducible. Consider, next, the following bounded invariant set (Dumont & Chiroleu, 2010):

$$\mathcal{B} = \left\{ (S_H, R_H, E_V, L_V, P_V, S_V, S_R, 0, 0, E_H, I_H, 0, 0, 0, I_V, E_R, I_R, T_R) \in \mathbb{R}_+^{18} : S_H \leq N_H^*, E_H \leq N_H^*, I_H \leq N_H^*, R_H \leq N_H^*, S_R \leq N_R^*, E_R \leq N_R^*, I_R \leq N_R^*, T_R \leq N_R^*, S_V \leq K_M, I_V \leq K_M \right\},$$

It is convenient to define

$$(\mathcal{R}_G)^2 = \frac{N_R^* K_M}{S_R^* S_V^*} (\mathcal{R}_2)^2 > (\mathcal{R}_2)^2.$$

Further, define a matrix $A_2(\bar{x}) = \bar{A}_2$, where \bar{A}_2 is an upper bound of the set (Elnaïem et al., 2001)

$$\mathcal{M} = \left\{ A_2(x) \in \mathbb{R}^{9 \times 9} : x(t) \in \mathcal{B} \right\},$$

with $\bar{x} = (N_H^*, 0, E_V^*, L_V^*(t), P_V^*, K_M, N_R^*, 0, 0, 0, 0, 0, 0, 0, 0, 0, 0, 0) \in \mathbb{R}_+^9 \times \{0\}$. It can be verified that $\rho(\bar{A}_2) \leq 0$ if and only if $\mathcal{R}_G \leq 1$. Thus, it follows from Theorem 2.7 in (Dumont & Chiroleu, 2010) that, for $\mathcal{R}_{EP} > 1$ and $\mathcal{R}_2 < 1$,

$$\begin{aligned} & (S_H(t), E_H(t), I_H(t), R_H(t), E_V(t), L_V(t), P_V(t), S_V(t), I_V(t), S_R(t), E_R(t), I_R(t), T_R(t)) \\ & \rightarrow \left(\frac{\Pi_H}{\mu_H}, 0, 0, 0, E_V^*, L_V^*, P_V^*, S_V^*, 0, \frac{\Pi_R}{\mu_R}, 0, 0, 0 \right), \text{ as } t \rightarrow \infty, \end{aligned} \tag{B-2}$$

where,

$$E_V^* = \frac{g_L + r_L L_V^*}{\sigma_E} I_V^*, P_V^* = \frac{\sigma_L I_V^*}{g_P} S_V^*, S_V^* = \frac{\sigma_L f \sigma_P I_V^*}{g_P g_M} L_V^*, L_V^* = \frac{1}{Q} \left(1 - \frac{1}{\mathcal{R}_{EP}} \right),$$

with $Q = \frac{g_E g_P g_M I_L}{\sigma_E \sigma_L f \sigma_P} + \frac{\psi_V \sigma_L f \sigma_P}{g_P g_M K_M}$, where $g_E = \sigma_E + \mu_E$, $g_L = \sigma_L + \mu_L + \xi_L$, $g_P = \sigma_P + \mu_P$ and $g_M = \mu_M + \xi_M$. Hence, the NDFE (\mathcal{E}_0) of the model (2.1), with $\delta_H = \delta_R = 0$, is GAS in $\Omega \setminus \{\mathcal{T}_0\}$ whenever $\mathcal{R}_{EP} > 1$ and $\mathcal{R}_2 < 1$.

References

Baneth, G., & Shaw, S. E. (2002). Chemotherapy of canine leishmaniosis. *Veterinary Parasitology*, 106, 315–324.

Bergsman, L. D., Hyman, J. M., & Manore, C. A. (2016). A mathematical model for the spread of West Nile virus in migratory and residents. *Mathematical Biosciences and Engineering*, 13, 401–424.

Bertholet, S., Goto, Y., Carter, L., Bhatia, A., Howard, R. F., Carter, D., et al. (2009). Optimized subunit vaccine protects against experimental leishmaniasis. *Vaccine*, 27, 7036–7045.

Blower, S. M., & Dowlatabadi, H. (1994). Sensitivity and uncertainty analysis of complex models of disease transmission: An HIV model, as an example. *International Statistical Review*, 2, 229–243.

Bowman, C., Gumel, A. B., van den Driessche, P., Wu, J., & Zhu, H. (2005). A mathematical model for assessing control strategies against West Nile virus. *Bulletin of Mathematical Biology*, 67, 1107–1133.

Burattini, M. N., Coutinho, F. A. B., Lopez, L. F., & Massad, E. (1998). Modelling the dynamic of leishmaniasis considering human, animal host and vector population. *Journal of Biological Systems*, 6, 337e356.

Canileish. <http://www.my-virbac.co.uk/file.aspx?id=317>. Accessed: February, 2017.

Carr, J. (1981). *Applications of Centre Manifold theory*. New York: Springer-Verlag.

Carvalho B. M., Rangel E. F., Ready P. D., Vale M. M.: Ecological Niche modelling predicts southward expansion of *lutzomyia (Nyssomyia) flaviscutellata* (Diptera: Psychodidae phlebotominae), vector of *Leishmania (Leishmania) amazonensis* in south America, under climate change. *PLoS One* . 10(11): e0143282. doi:10.1371/journal.pone.0143282.

Castillo-Chavez, C. C., & Song, B. (2004). Dynamical models of tuberculosis and their applications. *Mathematical Biosciences and Engineering*, 1, 361–404.

Centre of Epidemiological Surveillance of Sao Paulo State (CES-SP), Brazil. (2016). *Visceral Leishmaniasis reported data (only in Portuguese)*. http://www.cve.saude.sp.gov.br/htm/cve_leishvis.html. <http://www.cve.saude.sp.gov.br/> Accessed 17 Nov.

Chappuis, F., Sundar, S., Hailu, A., Ghalib, H., Rijal, S., Peeling, R. W., et al. (2007). Visceral leishmaniasis: What are the needs for diagnosis, treatment and control? *Nature Reviews Microbiology*, 5, 873–882.

Cruz-Pacheco, G., Esteva, L., & Vargas, C. (2012). Control measures for Chagas disease. *Mathematical Biosciences*, 237, 49–60.

Diekmann, O., Heesterbeek, J., & Metz, J. (1990). On the definition and the computation of the basic reproduction ratio R_0 in models for infectious diseases in heterogeneous populations. *Journal of Mathematical Biology*, 28, 365–382.

Dumont, Y., & Chiroleu, F. (2010). Vector control for the Chikungunya disease. *Mathematical Biosciences and Engineering*, 7, 105–111.

Elnaïem, D. A., Hassan, M. M., Maingon, R., Nureldin, G. H., Mekawi, A. M., Miles, M., et al. (2001). The Egyptian mongoose, *Herpestes ichneumon*, is a possible reservoir host of visceral leishmaniasis in eastern Sudan. *Parasitology*, 122, 531–536.

Espejo, L. A., Costard, S., & Zangmutt, F. J. (2015). Modelling canine leishmaniasis spread to non-endemic areas of Europe. *Epidemiology and Infection*, 143, 1936–1949.

European Centre for Disease Prevention and Control. <http://ecdc.europa.eu/en/healthtopics/vectors/sanflies/Pages/sandflies.aspx>. Accessed: February, 2017.

Forouzannia, F., & Gumel, A. B. (2014). Mathematical analysis of an age-structured model for malaria transmission dynamics. *Mathematical Biosciences*, 247, 80–94.

Garba, S. M., Gumel, A. B., & Abu Bakar, M. R. (2008). Backward bifurcations in dengue transmission dynamics. *Mathematical Biosciences*, 215, 11–25.

- Gillespie, P. M., Beaumier, C. M., Strych, U., Hayward, T., Hotez, P. J., & Bottazzi, M. E. (2016). Status of vaccine research and development of vaccines for leishmaniasis. *Vaccine*, *34*, 2992–2995.
- Hartemink, N., Vanwambeke, S. O., Heesterbeek, H., Rogers, D., Morley, D., Pesson, B., et al. (2011). Integrated mapping of establishment risk for emerging vector-borne infections: A case study of canine leishmaniasis in southwest France. *PLoS One*, *6*, e20817. <https://doi.org/10.1371/journal.pone.0020817>.
- Hoogstraal, H., & Heyneman, D. (1969). Leishmaniasis in the Sudan Republic. 30. Final epidemiologic report. *The American Journal of Tropical Medicine and Hygiene*, *18*, 1091–1210.
- Hussaini, N., Lubuma, J. M.-S., Barley, K., & Gumel, A. B. (2016). Mathematical analysis of a model for AVL–HIV co-endemicity. *Mathematical Biosciences*, *271*, 80–95.
- Kirk, R. (1939). Studies in leishmaniasis in the Anglo-Egyptian Sudan. Part I. - epidemiology and general considerations. *Transactions of the Royal Society of Tropical Medicine & Hygiene*, *32*, 533–544.
- Kumar, R., & Engwerda, C. (2014). Vaccines to prevent leishmaniasis. *Clinical & Translational Immunology*, *3*, e13.
- LaSalle, J. P. (1976). The stability of dynamical systems. In *regional conference series in applied mathematics*. Philadelphia: SIAM.
- Laurenti, M. D., Rossi, C. N., da Matta, V. L., Tomokane, T. Y., Corbett, C. E., et al. (2013). Asymptomatic dogs are highly competent to transmit Leishmania (Leishmania) infantum chagasi to the natural vector. *Veterinary Parasitology*, *196*, 296–300.
- Leta, S., Dao, T. H. T., Mesele, F., & Alemayehu, G. (2014). Visceral leishmaniasis in Ethiopia: An evolving disease. *PLoS Neglected Tropical Diseases*, *8*, e3131.
- Marini, G., Ros, R., Pugliese, A., & Heesterbeek, H. (2017). Exploring vector-borne infection ecology in multi-host communities: A case study of west Nile virus. *Journal of Theoretical Biology*, *415*, 58–69.
- Marino, S., Hogue, I. B., Ray, C. J., & Kirschner, D. E. (2008). A methodology for performing global uncertainty and sensitivity analysis in systems biology. *Journal of Theoretical Biology*, *254*, 178–196.
- McAllister, M. M. (2014). Successful vaccines for naturally occurring protozoal diseases of animals should guide human vaccine research. A review of protozoal vaccines and their designs. *Parasitology*, *141*, 624–640.
- Mckay, M. D., Beckman, R. J., & Conover, W. J. (1979). Comparison of 3 methods for selecting values of input variables in the analysis of output from a computer code. *Technometrics*, *21*, 239–245.
- McLeod, R. G., Brewster, J. F., Gumel, A. B., & Slonowsky, D. A. (2006). Sensitivity and uncertainty analyses for a SARS model with time-varying inputs and outputs. *Mathematical Biosciences and Engineering*, *2*, 527–544.
- Nagill, R., & Kaur, S. (2011). Vaccine candidates for leishmaniasis: A review. *International Immunopharmacology*, *11*, 1464–1488.
- Okuneye, K., Abdelrazec, A., & Gumel, A. B. (2018). Mathematical analysis of a weather-driven model for population ecology and dispersal of mosquitoes. *Mathematical Biosciences and Engineering*, *15*(1), 57–93.
- Okuneye, K., & Gumel, A. B. (2017). Analysis of a temperature- and rainfall-dependent model for malaria transmission dynamics. *Mathematical Biosciences*, *287*, 72–92.
- Parasites - Leishmaniasis. <https://www.cdc.gov/parasites/leishmaniasis/dogs.html>. Accessed: October, 2017.
- Parnell, N. K., Guptill, L., & Solano-Gallego, L. (2008). Protozoal Infections. In R. V. Morgan (Ed.), *Handbook of small animal practice* (5th ed., Vol. 116, pp. 1132–1146). Saint Louis: W.B. Saunders <https://www.sciencedirect.com/science/article/pii/B9781416039495501205>.
- PetCareRx. (July 17, 2013). *Lifespan of a dog: A dog years chart by breed.* (Accessed July 2016).
- Petersen, C. A. (2009). Leishmaniasis, an emerging disease found in companion animals in the United States. *Topics in Companion Animal Medicine*, *24*, 182–188.
- Petersen, C. A., & Barr, S. C. (2009). Canine leishmaniasis in North America: Emerging or newly recognized? *Veterinary Clinics of North America: Small Animal Practice*, *39*, 1065–1074.
- Poché, D. M., Grant, W. E., & Wang, H.-H. (2016). Visceral leishmaniasis on the Indian Subcontinent: Modelling the dynamic relationship between vector control schemes and vector life cycles. *PLoS Neglected Tropical Diseases*, *10*, e0004868.
- Podaliri Vulpiani, M., Iannetti, L., Paganico, D., Iannino, F., & Ferri, N. (2011). Methods of control of the Leishmania infantum dog reservoir: State of the art. *Veterinary Medicine International*, *2011*.
- Quinnell, R. J., & Courtenay, O. (2009). Transmission, reservoir hosts and control of zoonotic visceral leishmaniasis. *Parasitology*, *136*, 1915–1934.
- Ribas, L. M., Zaher, V. L., Shimozaiko, H. J., & Massad, E. (2013). Estimating the optimal control of zoonotic visceral leishmaniasis by the use of a mathematical model. *Science World Journal*, *2013*.
- Roberts, M. T. M. (2005). Current understandings on the immunology of leishmaniasis and recent developments in prevention and treatment. *British Medical Bulletin*, *75*, 115–130.
- Sand fly life cycle. <http://animals.mom.me/sand-fly-life-cycle-7392.html>. Accessed: February, 2017.
- Sharma, U.: Entomology Part-IV. <https://www.slideshare.net/jamesmacroony/entomology-louse-bedbugs>. Accessed: March, 2017.
- Shimozaiko, H. J., Wu, J., & Massad, E. (2017). Mathematical modelling for zoonotic visceral leishmaniasis dynamics: A new analysis considering updated parameters and notified human Brazilian data. *Infectious Disease Modelling*, *2*, 143–160.
- Smith, H. L. (1986). Competing subcommunities of mutualists and a generalized Kamke theorem. *SIAM Journal on Applied Mathematics*, *46*, 856–874.
- Srinivasan, R., & Panicker, K. N. (1992). Cannibalism among immatures of *Phlebotomus papatasi* (Diptera: Phlebotomidae). *Journal of the Bombay Natural History Society*, *89*, 386–387.
- Stauch, A., Sarkar, R. R., Picado, A., Ostyn, B., Sundar, S., et al. (2011). Visceral leishmaniasis in the Indian Subcontinent: Modelling epidemiology and control. *PLoS Neglected Tropical Diseases*, *5*, e1405. <https://doi.org/10.1371/journal.pntd.0001405>.
- Subramanian, A., Singh, V., & Sarkar, R. R. (2015). Understanding visceral leishmaniasis disease transmission and its control - a study based on mathematical modeling. *Mathematics*, *3*, 913–944.
- The Africa Report. (March 8, 2013). Ethiopia: Mass dog killing concerns hit Addis Ababa. Retrieved July 30, 2016 <http://www.theafricareport.com/East-Horn-Africa/ethiopia-mass-dog-killing-concerns-hit-addis-ababa.html>. (Accessed September 2017).
- Van den Driessche, P., & Watmough, J. (2002). Reproduction numbers and sub-threshold endemic equilibria for compartmental models of disease transmission. *Mathematical Biosciences*, *180*, 29–48.
- Vetlife. Leishmaniasis. <http://www.vet4life.co.uk/leishmaniasis/>. Accessed: February, 2017.
- World Bank Data (2015). <http://data.worldbank.org/country/brazil>. Accessed: Nov, 2017.
- World Health Organization. Leishmaniasis. <http://www.who.int/mediacentre/factsheets/fs375/en/>. (Accessed February 2017).
- Zhao, S., Kuang, Y., Wu, C.-H., Ben-Arieh, D., Ramalho-Ortigao, M., & Bi, K. (2016). Zoonotic visceral leishmaniasis transmission: Modeling, backward bifurcation, and optimal control. *Journal of Mathematical Biology*, *73*, 1525–1560.